Nonlinear Dyn (2011) 64: 25–47
DOI 10.1007/s11071-010-9843-y

ORIGINAL PAPER

A new model for dry and lubricated cylindrical joints with clearance in spatial flexible multibody systems

Qiang Tian · Cheng Liu · Margarida Machado · Paulo Flores

Received: 10 May 2010 / Accepted: 14 September 2010 / Published online: 9 October 2010

Abstract A new approach to model and analyze flexible spatial multibody systems with clearance of cylindrical joints is presented in this work. The flexible parts are modeled by using absolute nodal coordinate formulation (ANCF)-based elements, while the rigid parts are described by employing the natural coordinate formulation (NCF), which can lead to a constant system mass matrix for the derived system equations of motion. In a simple way, a cylindrical joint with clearance is composed of two main elements, that is, a journal inside a bearing. Additionally, a lubricant fluid can exist between these two mechanical elements to reduce the friction and wear and increase the system's life. For the case in which the joint is modeled as a dry contact pair, a technique using a continuous approach for the evaluation of the contact force is applied, where the energy dissipation in the form of hysteresis damping is considered. Furthermore, the frictional forces developed in those contacts are evaluated by using a modified Coulomb's friction law. For the lubricated case, the hydrodynamic theory for dynamically loaded journal bearings is used to compute the forces generated by lubrication actions. The lubricated model is based on the Reynolds equation developed for the case of journal bearings with length-to-diameter ratios up to 1. Using this approach, the misalignment of the journal inside the bearing can be studied. Finally, two demonstrative examples of application are used to provide results that support the discussion and show the validity of the proposed methodologies.

Keywords Clearance cylindrical joint · Absolute nodal coordinate formulation (ANCF) · Natural coordinate formulation (NCF) · Dry contact forces · Lubrication forces · Journal misalignment

Q. Tian (✉) · C. Liu
Department of Mechanics, School of Aerospace Engineering, Beijing Institute of Technology, Beijing 100081, China
e-mail: tianqiang_hust@yahoo.com.cn

M. Machado · P. Flores
Department of Mechanical Engineering, University of Minho, Campus de Azurém, 4800-058 Guimarães, Portugal

M. Machado
e-mail: margarida@dem.uminho.pt

P. Flores
e-mail: pflores@dem.uminho.pt

1 Introduction

It is well known that the classical dynamic analysis of spatial multibody systems does not take into account factors such as flexibility of the bodies or clearance in the joints [1–3]. In fact, clearances are inevitable and necessary to allow for the assembly and correct functioning conditions of the pair elements. Other reasons for the existence of the clearances in mechanical systems are manufacturing tolerances [4], wear [5], thermal effects [6], and local deformations [7]. As a consequence, the contact–impact forces developed at the clearance joints can greatly affect the dynamic responses of the system and eventually lead to important deviations from their ideal outcome [8–10]. Moreover, the contact–impact phenomenon causes high-frequency vibration and joint wear, which will further reduce the mechanisms performance and service life.

Over the last few decades a significant number of research works have proposed several approaches to model and analyze multibody systems with clearance joints [11–20]. However, the range of application of most of these works is somewhat restricted in the sense that they are valid for planar multibody systems with dry clearance joints. In the most general case of multibody systems, the motion allowed is in the spatial domain, as is the case of vehicle models, car suspension, and robotic manipulators. Tian et al. [21] and Flores and Lankarani [22] are among the very few that modeled spatial multibody systems with lubricated spherical joints. In fact, one of the most commonly used solutions to avoid or reduce the metal-to-metal contact within the clearance joints is to include a fluid lubricant between the joint elements. Some relevant research works on multibody systems with lubricated joints for planar applications have been presented. Roger and Andrews [23] developed a two-dimensional mathematical model for the journal-bearing elements which takes into account the effect of clearance, surface compliance, and lubrication. However, their lubrication model only accounts for the squeeze-film effect. Liu and Lin [24] extended Roger and Andrews' work to include both squeeze-film and wedge-film actions. Ravn et al. [25] proposed a modified force model for the lubricated long bearings in the multibody systems. Schwab et al. [26], basing their work on that of Moes et al. [27], applied the impedance method to model lubricated revolute joints in a slider-crank mechanism. More recently, Flores and co-workers [28], in a very complete paper, compared the effect of different lubrication force models on dynamic response of the rigid multibody systems with lubricated planar revolute joints. Tian et al. [29] extended the work of Flores et al. to include the effect of the flexibility of the bodies in multibody systems including lubricated joints. Stefanelli et al. [30] investigated the dynamic behavior of the rigid rotor system with lubricated cylindrical joints in which the journal misalignment was taken into account. However, this work was only applied to isolated journal-bearing systems.

The main goal of this work is to present a new approach for dynamic analysis of flexible spatial multibody mechanical systems that include cylindrical joints with clearance and lubrication effects. In the sequel of this process, the main issues associated with the absolute nodal coordinate formulation (ANCF) and natural coordinate formulation (NCF) are reviewed. In the classical analysis of a cylindrical joint the journal and bearing share the same axis; that is, the cylindrical joint is considered to be ideal or perfect. The inclusion of the clearance separates the two bodies and, therefore, the joint is not ideal anymore. Indeed, from a practical point of view, some amount of clearance is always present in the joints in order to allow the relative motion between the journal and the bearing. When compared with an ideal joint modeled by a set of kinematic constraints, four extra degrees of freedom are added to the system for a model with a cylindrical clearance joint. Hence, an actual cylindrical joint does not impose kinematic constraints as in the ideal case; instead it deals with force constraints. If there is no lubricant, the journal can move freely within the bearing until contact between the two bodies takes place. Thus, for the case of the joints with clearance modeled as a dry contact pair, a technique using a continuous approach for the evaluation of the contact force is applied, in which the energy dissipation in form of hysteresis damping is considered. The friction forces are calculated using a modified Coulomb's friction law. For the lubricated case, the hydrodynamic theory for dynamically loaded journal bearings is used to compute the forces generated by lubrication actions. Both squeeze and wedge hydrodynamic effects are included in the dynamically loaded journal-bearings formulation. In a simple way, the forces built up by the lubricant fluid are evaluated from the state of variables of the system and included into the equations of motion of the multibody system.

The remainder of this paper is organized as follows. In Sect. 2, the main kinematic aspects of the cylindrical clearance joints are presented, which are based on the ANCF and NCF approaches. Section 3 deals with the general methodology used to evaluate the dry contact and lubrication forces produced in the cylindrical joints with clearance, within the framework of the multibody systems formulation. Section 4 introduces an efficient computational strategy for the solution of the equations of motion for constrained flexible spatial multibody systems that include cylindrical clearance joint with both dry and lubrication actions. Section 5 provides two numerical examples of application, namely a spatial double pendulum and a spatial slider-crank mechanism, which incorporate perfect, clearance and lubricated cylindrical joints. The global results produced with the proposed methodology are compared with the data published in the thematic literature. In addition, the commercial software MSC.ADAMS was also used to compare and validate the proposed model for the case of stiff systems. Finally, in the last section the main conclusions from this study are drawn and the perspectives for future research are outlined.

2 Kinematics of cylindrical joints with clearance

2.1 Geometrical definition

In a standard cylindrical kinematic joint, it is assumed that the axis of the journal and bearing parts are parallel to each other. The introduction of the clearance in a cylindrical joint allows for relative motion between the journal and bearing. Figure 1a depicts a cylindrical joint with clearance, that is, the journal bearing, where the difference in radius between the bearing and journal defines the radial clearance. The clearance in a realistic connection is much smaller than the length of the two cylinders and of the nominal radius of the elements connected by the joint. Thus, this type of joint does not constrain any degree of freedom from a mechanical system, as in the perfect joint case. Instead, it imposes some restrictions on the limit journal motion inside the bearing, the dynamics of the joint controlled by contact–impact forces of different nature that develop when the journal and bearing surfaces move relative to each other. Therefore, mechanical joints with clearance can be called force joints instead of kinematic joints.

Figure 1b shows a cylindrical joint with clearance that connects two flexible links. The journal and bearing elements are considered to be rigid bodies. The geometric center of the bearing is represented by point P. In the present study, a rigid body is described by the NCF approach, that is, two points and two unit non-coplanar vectors. For the example, the journal is characterized by two points A_j and W_j, and two unit non-coplanar vectors $\mathbf{U}_j$ and $\mathbf{V}_j$, as is illustrated in Fig. 1b. Thus, any rigid body is totally described in the global coordinate framework when a set of 12 coordinates is used. In turn, the position of the bearing is completely determined by using 12 Cartesian coordinates relative to points A_b, W_b, and vectors $\mathbf{U}_b$ and $\mathbf{V}_b$, which can be compacted in the form $[\mathbf{r}_{W_b}^{\mathrm{T}}\ \mathbf{r}_{A_b}^{\mathrm{T}}\ \mathbf{U}_b^{\mathrm{T}}\ \mathbf{V}_b^{\mathrm{T}}]^{\mathrm{T}}$. At this stage it is important to note that this approach will lead to a constant mass matrix for the final derived rigid body equations of motion [31].

As far as the flexible beam is concerned, the original two nodes 3D ANCF-based beam element developed by Shabana and Yakoub [32, 33] is used in the kinematic description. Although this element will suffer shear or Poisson locking problems, it is quite easy to extend this element to other types of spatial locking-

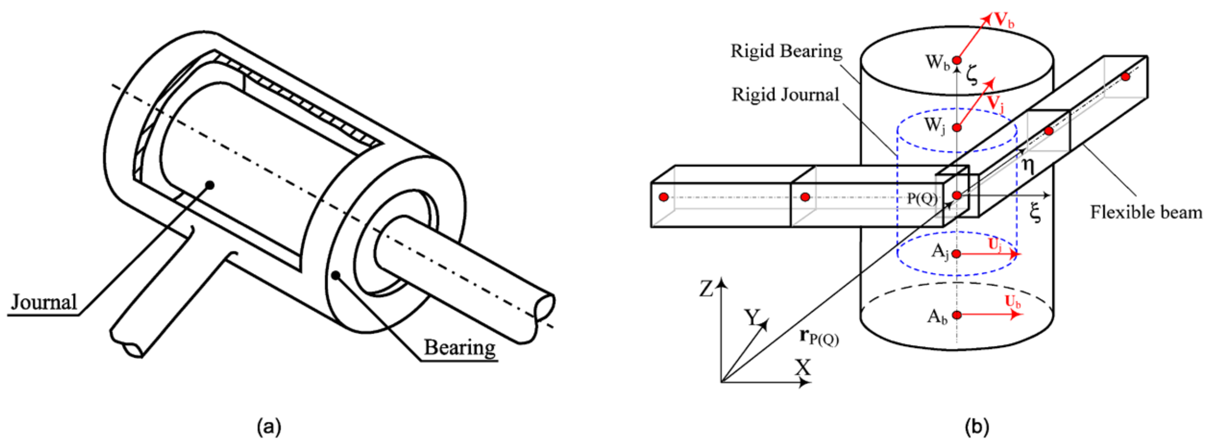

Fig. 1 (**a**) Typical representation of a cylindrical joint with clearance; (**b**) kinematic description for the cylindrical clearance with joint based on ANCF and NCF

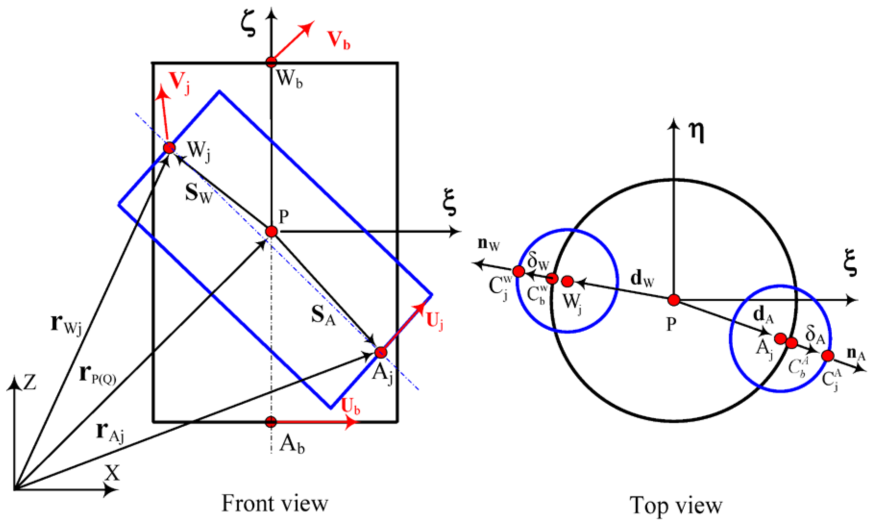

Fig. 2 Front and top views of the top and bottom journal bases at the point of contact with the bearing wall

free ANCF-based beam elements, whose formulation only differs from the original elements in the approach of the elastic forces [34, 35]. In addition, the locking problems associated with this element can be avoided or, at least, reduced by increasing the number of elements used in the discretization of the flexible part. Thus, the global position of an arbitrary point in the 3D ANCF-based element can be determined by considering the nodal coordinates vector **e** with 24 coordinates [32, 33]

$$\mathbf{r} = \mathbf{S}\mathbf{e} \tag{1}$$

in which **S** is the used beam element shape function. Since the NCF and ANCF approaches can lead to constant mass matrix for the equations of motion of rigid and flexible bodies, respectively, the resulting system mass matrix for the rigid-flexible systems will also be constant, which will increase the computational efficiency. In addition, since the slope vector coordinates, describing the beam element cross section deformation and rotation, and the unit vector coordinates, describing the rigid body rotation, coexist in the final multibody system equations of motion, the constraint equations can be significantly simplified [36].

2.2 Mathematical model

In order to include the intra-joint contact–impact forces into the equations of motion for spatial flexible multibody systems based on the mixed formulation (ANCF and NCF), it is first necessary to develop a mathematical model for cylindrical joints with clearance. For this purpose, let us consider Fig. 2, in which both top and bottom journal bases contact with the bearing wall.

It should be highlighted that the derived formulation presented in what follows is based on the assumption of journal small rotation, because the clearance is in general very small when compared with the journal-bearing geometry. Based on the NCF, all the rigid body coordinates are defined in the global coordinate system; then the vectors $\mathbf{S}_W$ and $\mathbf{S}_A$ can be written as follows:

$$\mathbf{S}_W = \mathbf{r}_{W_j} - \mathbf{r}_P \tag{2}$$

$$\mathbf{S}_A = \mathbf{r}_{A_j} - \mathbf{r}_P \tag{3}$$

From the top view, the eccentricity vectors at the top and bottom journal bases, $\mathbf{d}_W$ and $\mathbf{d}_A$, can be obtained by projecting vectors $\mathbf{S}_W$ and $\mathbf{S}_A$ onto the local axes ξ and η, yielding

$$\mathbf{d}_W = (\mathbf{S}_W \cdot \mathbf{U}_b)\mathbf{U}_b + (\mathbf{S}_W \cdot \mathbf{V}_b)\mathbf{V}_b \tag{4}$$

$$\mathbf{d}_A = (\mathbf{S}_A \cdot \mathbf{U}_b)\mathbf{U}_b + (\mathbf{S}_A \cdot \mathbf{V}_b)\mathbf{V}_b \tag{5}$$

The eccentricity vectors are expressed in the global coordinate system because the bearing local coordinate framework $\xi\eta\zeta$ is completely determined by knowing the unit vectors $\mathbf{U}_b$ and $\mathbf{V}_b$ defined in the global coordinate system XYZ. Then, the magnitudes of the eccentricity vectors are computed by using the

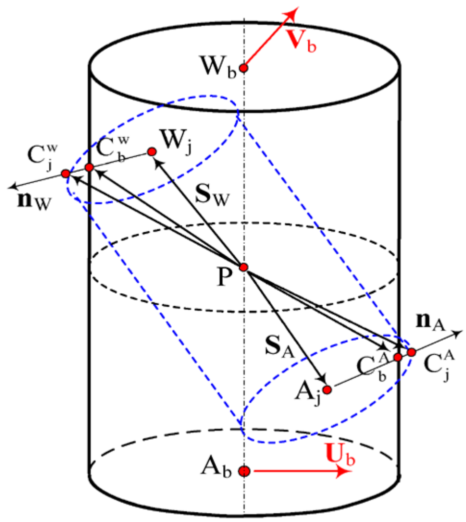

Fig. 3 The position of the contact points on the rigid journal and bearing

following relations:

$$d_W = \sqrt{(\mathbf{S}_W \cdot \mathbf{U}_b)^2 + (\mathbf{S}_W \cdot \mathbf{V}_b)^2} \tag{6}$$

$$d_A = \sqrt{(\mathbf{S}_A \cdot \mathbf{U}_b)^2 + (\mathbf{S}_A \cdot \mathbf{V}_b)^2} \tag{7}$$

The unit vectors $\mathbf{n}_W$ and $\mathbf{n}_A$ shown in the top view of Fig. 2, normal to the planes of contact where the top and bottom journal bases touch the bearing wall, can be evaluated as

$$\mathbf{n}_W = \frac{\mathbf{d}_W}{d_W} \tag{8}$$

$$\mathbf{n}_A = \frac{\mathbf{d}_A}{d_A} \tag{9}$$

In regard to Fig. 2, the penetrations due to the contact between the journal bases and bearing wall are calculated as

$$\delta_W = d_W - c \tag{10}$$

$$\delta_A = d_A - c \tag{11}$$

where c is the radial clearance. Figure 3 gives a detailed representation of the contact points on the rigid journal and bearing elements.

The global positions of the potential contact points C_j^W, C_b^W, C_j^A and C_b^A on the rigid journal and bearing can be evaluated as

$$\mathbf{r}^{C_j^W} = \mathbf{r}_{W_j} + R_j \mathbf{n}_W \tag{12}$$

$$\mathbf{r}^{C_b^W} = \mathbf{r}_P + R_b \mathbf{n}_W + (S_W)_Z \tag{13}$$

$$\mathbf{r}^{C_j^A} = \mathbf{r}_{A_j} + R_j \mathbf{n}_A \tag{14}$$

$$\mathbf{r}^{C_b^A} = \mathbf{r}_P + R_b \mathbf{n}_A + (S_A)_Z \tag{15}$$

where $(\mathbf{S}_W)_Z$ and $(\mathbf{S}_A)_Z$ denote the components of vectors $\mathbf{S}_W$ and $\mathbf{S}_A$ in the Z-direction, respectively. Thus, the relative impact velocities can be evaluated by

$$\Delta\dot{\mathbf{r}}^W = \dot{\mathbf{r}}^{C_j^W} - \dot{\mathbf{r}}^{C_b^W} \tag{16}$$

$$\Delta\dot{\mathbf{r}}^A = \dot{\mathbf{r}}^{C_j^A} - \dot{\mathbf{r}}^{C_b^A} \tag{17}$$

The relative velocities of the contact points are projected onto the direction of the penetration, yielding the relative contact normal velocities, $\dot{\boldsymbol{\delta}}^W$ and $\dot{\boldsymbol{\delta}}^A$, as

$$\dot{\boldsymbol{\delta}}^W = \left(\Delta\dot{\mathbf{r}}^W\right)^T \mathbf{n}_W \tag{18}$$

$$\dot{\boldsymbol{\delta}}^A = \left(\Delta\dot{\mathbf{r}}^A\right)^T \mathbf{n}_A \tag{19}$$

Finally, the relative tangential velocities, $\mathbf{V}_t^W$ and $\mathbf{V}_t^A$, are calculated by

$$\mathbf{V}_t^W = \Delta\dot{\mathbf{r}}^W - \dot{\boldsymbol{\delta}}^W \tag{20}$$

$$\mathbf{V}_t^A = \Delta\dot{\mathbf{r}}^A - \dot{\boldsymbol{\delta}}^A \tag{21}$$

From all the above formulations, it can be seen that the coordinate transformation skills are no longer needed because all the coordinates are defined in the global coordinate framework, which leads to much simpler formulation expressions than those in the work [37].

3 Dynamics of cylindrical joints with clearance

3.1 Dry contact forces

In order to evaluate efficiently the contact forces developed between the bearing and journal, in a cylindrical joint with clearance, special attention must be given to the numerical description of the contact model. Information on the impact velocity, material properties of the colliding bodies, and geometric characteristics of the surfaces in contact must be included into the contact force model. These characteristics are observed with a continuous contact force, in which the deformation and contact force are considered as continuous functions. Furthermore, it is important that the contact model add to the stable integration of the multibody system's equation of motion [38–40]. In the present study, the interaction between the journal and bearing is modeled by using the continuous contact force model proposed by Lankarani and Nikravesh [41], which is given by

$$F_n = K\delta^{\alpha}\left[1+\frac{3(1-c_e^2)}{4}\frac{\dot{\delta}}{\dot{\delta}^{(-)}}\right] \tag{22}$$

where K represents the generalized stiffness parameter, δ is the relative normal deformation or penetration depth between the contacting bodies, c_e is the coefficient of restitution, $\dot{\delta}$ represents the relative normal contact velocity, and $\dot{\delta}^{(-)}$ is the initial impact velocity. The exponent α is typically equal to $3/2$, but can also assume other values [42, 43]. The generalized parameter K is dependent on the material properties and the shape of the surfaces in contact and can be evaluated as [44]

$$K = \frac{4}{3(\sigma_j+\sigma_b)}\left[\frac{R_b R_j}{R_b - R_j}\right]^{1/2} \tag{23}$$

in which σ_j and σ_b denote the material parameter for rigid journal and bearing, respectively, which are given by

$$\sigma_k = \frac{1-\upsilon_k^2}{E_k} \quad (k = j, b) \tag{24}$$

where υ_k and E_k are the Poisson ratio and the material Young's modulus associated with the corresponding body, respectively.

It is important to highlight that the contact force model given by (22) is only valid for impact velocities lower than the propagation speed of elastic waves across the bodies [41, 45–47]. Readers interested in this particular issue are referred to some relevant research works that offer a detailed discussion on different approaches to model and analyze contact–impact events within the spirit of multibody systems methodologies [48–53].

In a broad sense, in dynamic analysis of the multibody systems with clearance joints, the friction is a quite complex phenomenon which involves interaction between the surfaces of contacting bodies and may lead to different friction regimes such as sliding and stiction [54]. During the impact process, the friction force models and corresponding coefficients will affect the simulation accuracy significantly. The most widely used and simplest friction force model is the well-known Coulomb friction law [55], in which the magnitude of the friction force is proportional to the normal contact force. However, for the dynamic analysis of the multibody system with clearance joints, it has been demonstrated that Coulomb's friction model will pose some numerical difficulties, which in turn may lead to simulation divergence. To avoid this problem, a modified Coulomb friction law is used [56],

$$\mathbf{F}_t = -c_f c_d F_n \frac{\mathbf{v_t}}{\|\mathbf{v_t}\|} \tag{25}$$

where c_f is the friction coefficient and the dynamic correction coefficient c_d is given by

$$c_d = \begin{cases} 0 & \text{if } \|\mathbf{v}_t\| \le \upsilon_0 \\ \frac{\|\mathbf{v}_t\|-\upsilon_0}{\upsilon_1-\upsilon_0} & \text{if } \upsilon_0 \le \|\mathbf{v}_t\| \le \upsilon_1 \\ 1 & \text{if } \|\mathbf{v}_t\| \ge \upsilon_1 \end{cases} \tag{26}$$

where υ_0 and υ_1 are specified tolerances for the relative tangential velocity of the surfaces in contact. The great merit of the modified Coulomb law expressed by (25) is that it allows the numerical stabilization of the integration algorithm. It can be observed that this friction force model does not account for other tribological phenomena like the adherence between the sliding contact surfaces. Furthermore, the disadvantage when using a friction model such as (25), for simulation or control purposes, is the problem of detecting when the relative tangential velocity is zero. A solution for this problem is found in the model proposed by Karnopp, which was developed to overcome the problems with zero velocity detection and to avoid switching between different state equations for sticking and sliding [57]. The drawback of this model is that it is very strongly coupled with the rest of the system. The external force is an input to the model and this force is not always explicitly given. Variations of the Karnopp model are widely used since they allow efficient simulations, such as the modified Karnopp model by Centea et al. [58] and the reset integrator model by Haessig and Friedland [59].

Figure 4 shows the representation of the friction force and moment that act on the journal surface when it contacts with the bearing surface. The value of the friction moment can be evaluated as

$$\mathbf{M}_t^W = \mathbf{F}_t^W \otimes R_j \mathbf{n} \tag{27}$$

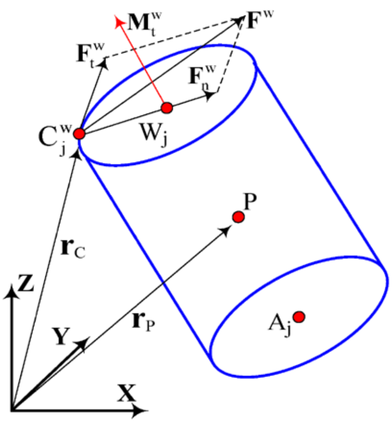

Fig. 4 The friction force and friction moment that act on the journal element

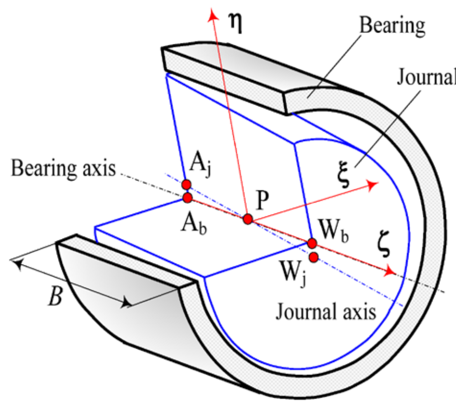

Fig. 5 Generic configuration of a lubricated cylindrical joint with journal misalignment

where the symbol ⊗ denotes the cross product operator.

It should be noted that, due to the fact that all the coordinates for the rigid journal element are full Cartesian coordinates based on the NCF, the friction moment cannot be applied directly on the journal. Instead, it has to be transformed into an equivalent pair of forces of equal magnitude and opposite directions. Readers interested in this topic are referred to the textbook by García de Jalón and Bayo [60].

3.2 Hydrodynamic lubrication forces

This section deals with the evaluation of the hydrodynamic forces that develop in a lubricated cylindrical joint. It can be said that a suitable lubrication system can prevent direct dry contact phenomena and, consequently, reduce wear and extend the service life of the mechanical systems. Therefore, proper modeling of multibody systems with lubricated joints is required to achieve a better understanding of their dynamic performance. Figure 5 shows the generic configuration of a typical lubricated cylindrical joint, in which the journal misalignment is also represented. In a similar way to the case of the dry contact situation, the bearing center of mass is denoted by point P, the journal-bearing length being represented by B. The local coordinate system is denoted by $\xi\eta\zeta$.

Figure 6 depicts an arbitrary journal cross section along the ζ axis, which is used to describe the general methodology presented to determine the hydrodynamic forces.

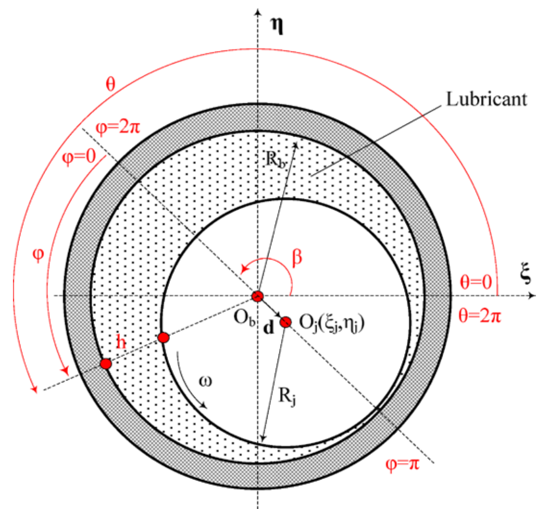

Fig. 6 Cross section of the lubricated cylindrical joint

With regard to Fig. 6, the general form of the isothermal Reynolds equation can be expressed as [61]

$$\frac{1}{R_j^2}\frac{\partial}{\partial\varphi}\left(h^3\frac{\partial p}{\partial\varphi}\right)+\frac{\partial}{\partial\zeta}\left(h^3\frac{\partial p}{\partial\zeta}\right)$$
$$=6\mu\omega\frac{\partial h}{\partial\varphi}+12\mu\frac{\partial h}{\partial t} \tag{28}$$

where p denotes the lubricant pressure, μ is the dynamic lubricant viscosity, and the lubricant film thickness, h, is given by

$$h=c+d\cos\varphi=c+d\cos(\theta-\beta) \tag{29}$$

in which c is the radial clearance and d represents the journal-bearing eccentricity.

When the journal misalignment is taken into account, the coordinates and the time derivatives of an arbitrary journal cross section along the ζ axis are expressed as functions of the local coordinates of points $A_j(\xi_1, \eta_1, -B/2)$ and $W_j(\xi_2, \eta_2, B/2)$ as follows:

$$
\begin{aligned}
\xi_j &= \xi_2 + \frac{(\xi_2 - \xi_1)(\zeta - B/2)}{B} \\
\eta_j &= \eta_2 + \frac{(\eta_2 - \eta_1)(\zeta - B/2)}{B} \\
\dot{\xi}_j &= \dot{\xi}_2 + \frac{(\dot{\xi}_2 - \dot{\xi}_1)(\zeta - B/2)}{B} \\
\dot{\eta}_j &= \dot{\eta}_2 + \frac{(\dot{\eta}_2 - \dot{\eta}_1)(\zeta - B/2)}{B}
\end{aligned}
\tag{30}
$$

Substituting (30) into (29) yields the lubricant film thickness for the case of the misaligned journal as

$$
\begin{aligned}
h &= c + d\cos\varphi = c + d\cos(\theta - \beta) \\
&= c - \xi_j \cos\theta - \eta_j \sin\theta
\end{aligned}
\tag{31}
$$

where θ is the angular coordinate of the journal bearing and the variable β is given by

$$
\beta = \tan^{-1}\left(\frac{\eta_j}{\xi_j}\right) \tag{32}
$$

It is well known that the exact solution of the Reynolds equation is quite difficult to obtain and, in general, requires a considerable numerical effort [62]. However, it is possible to solve the Reynolds equation analytically by assuming either the first or the second term on the left-hand side of (28) to be null. These solutions correspond to infinitely short and infinitely long journal bearings, respectively [63]. In the most usual engineering applications, the journal bearings are considered to be short, which reduces uneven axial load distribution and frictional loss. This assumption is valid for length-to-diameter ratios up to 1.0. Hence, the Reynolds equation for an infinitely short journal bearing is written as [30, 61]

$$
\begin{aligned}
h^3 \frac{\partial^2 p}{\partial \zeta^2} &= 6\mu\omega \frac{\partial h}{\partial \varphi} + 12\mu \frac{\partial h}{\partial t} \\
&= -6\mu\omega d \sin\varphi + 12\mu \frac{\partial h}{\partial t} \\
&= -6\mu\omega d \sin(\theta - \beta) + 12\mu \frac{\partial h}{\partial t}
\end{aligned}
\tag{33}
$$

The time derivative of the lubricant film thickness can be obtained from (31), yielding

$$
\frac{\partial h}{\partial t} = -\dot{\xi}_j \cos\theta - \dot{\eta}_j \sin\theta \tag{34}
$$

Using (33) and (34) and after some basic mathematical manipulation it is possible to write the following expression:

$$
\frac{\partial^2 p}{\partial \zeta^2} = \frac{6\mu[\omega(\xi_j \sin\theta - \eta_j \cos\theta) - 2(\dot{\xi}_j \cos\theta + \dot{\eta}_j \sin\theta)]}{(c - \xi_j \cos\theta - \eta_j \sin\theta)^3} \tag{35}
$$

Then, integrating (35) twice yields an expression that allows the evaluation of the pressure distribution for an arbitrary journal cross section with center O_j as

$$
\begin{aligned}
p(\theta, \zeta) = \frac{3\mu z^2}{h^3} \big[&\omega(\xi_j \sin\theta - \eta_j \cos\theta) \\
&- 2(\dot{\xi}_j \cos\theta + \dot{\eta}_j \sin\theta) \big] \\
&+ C_1 z + C_0
\end{aligned}
\tag{36}
$$

where C_0 and C_1 are the integrating constants, which can be obtained by taking into account the conditions that consider the film breakdown. These boundary conditions are expressed as

$$
\begin{cases}
p = 0 & \text{if } \zeta = -B/2 \\
p = 0 & \text{if } \zeta = B/2
\end{cases}
\tag{37}
$$

Thus, using these boundary conditions, the final pressure expression is given by

$$
\begin{aligned}
p(\theta, \zeta) = \frac{3\mu(4\zeta^2 - B^2)}{4h^3} \big[&\omega(\xi_j \sin\theta - \eta_j \cos\theta) \\
&- 2(\dot{\xi}_j \cos\theta + \dot{\eta}_j \sin\theta) \big]
\end{aligned}
\tag{38}
$$

It is convenient to determine the force components of the resultant pressure that act at the journal center of mass P. Thus, these force components can be expressed as

$$
F_\xi = -\int_{-B/2}^{B/2} \int_0^{2\pi} p(\theta, \zeta) R_j \cos\theta \, d\theta \, d\zeta \tag{39}
$$

$$
F_\eta = -\int_{-B/2}^{B/2} \int_0^{2\pi} p(\theta, \zeta) R_j \sin\theta \, d\theta \, d\zeta \tag{40}
$$

In a similar way, the resulting moment that acts at the journal center of mass P should be accounted for.

This moment is related to the friction torque due to the lubricant friction force

$$M_\xi = -\int_{-B/2}^{B/2}\int_0^{2\pi} p(\theta,\zeta) R_j \zeta \sin\theta \,\mathrm{d}\theta \,\mathrm{d}\zeta \tag{41}$$

$$M_\eta = \int_{-B/2}^{B/2}\int_0^{2\pi} p(\theta,\zeta) R_j \zeta \cos\theta \,\mathrm{d}\theta \,\mathrm{d}\zeta \tag{42}$$

Finally, the resulting forces and moments are obtained by numerical integration of (39)–(42). For this purpose, the pressure field is considered only over the positive part by setting the pressure in the remaining portion equal to zero. This boundary condition, associated with the pressure field, corresponds to Gümbel's boundary conditions [28, 63].

4 Computational strategy to solve the equations of motion

In the present study, the absolute nodal coordinate formulation (ANCF) and the natural coordinate formulation (NCF) are used to model and analyze the dynamic response of spatial multibody systems with cylindrical clearance joints. The ANCF approach is used to model the flexible parts, while the NCF is considered to model the rigid elements. The equations of motion for constrained flexible multibody systems can be expressed in a compact form as a set of differential and algebraic equations as [64]

$$\begin{cases} \mathbf{M}\ddot{\mathbf{q}} + \boldsymbol{\Phi}_{\mathbf{q}}^{\mathrm{T}}\boldsymbol{\lambda} + \mathbf{F}(\mathbf{q}) = \mathbf{Q}(\mathbf{q}) \\ \boldsymbol{\Phi}(\mathbf{q},t) = \mathbf{0} \end{cases} \tag{43}$$

where $\mathbf{M}$ is the system mass matrix, $\boldsymbol{\Phi}(\mathbf{q},t)$ represents the vector that contains the system constraint equations, $\boldsymbol{\Phi}_{\mathbf{q}}$ is the derivative matrix of constraint equations with respect to the system generalized coordinates $\mathbf{q}$, vector $\boldsymbol{\lambda}$ is the Lagrangian multipliers associated with the constraints, and $\mathbf{Q}(\mathbf{q})$ denotes the system external generalized forces. In this formulation, vector $\mathbf{Q}(\mathbf{q})$ includes the distributed gravitational forces as well as the contact–impact forces and the lubrication forces, and $\mathbf{F}(\mathbf{q})$ denotes the system elastic force vector. As has already been mentioned, based on the mixed formulations (ANCF and NCF), the system mass matrix $\mathbf{M}$ will be constant and the constraint equations can be simplified.

There are several methods for solving (43), namely those available in the specialized literature [65–67]. However, the process of solving the equations of motion in the case of systems with perfect joints differs from that for systems that include joints with clearances. This is mainly due to the high-frequency system dynamic responses associated with the contact–impact events that developed at the clearance joints, which ultimately lead to contact–impact forces with spurious high frequency and extremely large magnitude, even simulation divergence. Thus, in this work the generalized-$\boldsymbol{\alpha}$ method is used [68], which can dissipate the spurious system high-frequency responses and preserve the low-frequency responses very well. It should be highlighted that during the iteration process the elastic forces are efficiently evaluated by the first Piola–Kirchhoff stress tensor-based formulation proposed by Gerstmayr and Shabana [69] and the tangent matrix of the elastic force is calculated by using the numerical differentiation method [70].

As mentioned above, when the contact between journal and bearing is detected, the intra-joint contact–impact forces are evaluated and introduced into (43). In this process, the detection of the precise instant of contact is of crucial importance. The detection of the instant of contact takes place when the sign of penetration changes between the two discrete instants in time, t_n and t_{n+1}. Therefore, by monitoring the sign of the penetration at every time step, the instant of contact can be identified from

$$\delta\big(\mathbf{q}(t_n)\big)\cdot\delta\big(\mathbf{q}(t_{n+1})\big) \le 0 \tag{44}$$

When (44) is satisfied, the start of contact is defined as occurring at t_{n+1}. In a broad sense, such an accurate instant in time can be found by using the Newton–Raphson method [71]. In this study, in order to improve the computation efficiency, a fast and accurate third-order interpolation approach proposed by Meijaard [72] was used:

$$\begin{aligned}\mathbf{q}(t) = {} & \big(1-3\chi^2+2\chi^3\big)\mathbf{q}(t_n) \\ & + \big(\chi-2\chi^2+\chi^3\big)\Delta t\dot{\mathbf{q}}(t_n) \\ & + \big(3\chi^2-2\chi^3\big)\mathbf{q}(t_{n+1}) \\ & + \big(-\chi^2+\chi^3\big)\Delta t\dot{\mathbf{q}}(t_{n+1})\end{aligned} \tag{45}$$

where $\chi = (t-t_n)/\Delta t$ and $\Delta t = t_{n+1}-t_n$. Using this approach the instant of contact can be determined within a given error tolerance. It should be noted that, for the dry contact approach, the integration time step is not fixed because of the necessity to detect the precise instant of contact. For instance, if the time step selected by the user is too large, when the first impact is detected it will cause a large penetration, which, in turn, will cause artificially large contact forces that are not realistic [71]. Thus, in the present work, the contact detection is performed by using (45) due to the accuracy and computational efficiency introduced [72]. This approach has been successfully used by other researchers, such as Schwab et al. [26] and Tian et al. [29] for the dynamic analysis for planar multibody system with clearance joints.

5 Results and discussion

5.1 Spatial double pendulum

The effectiveness of the formulations presented in this work is demonstrated through the use of a spatial double pendulum with the initial configuration illustrated in Fig. 7. This double pendulum is composed of four bodies, two rigid journals and two flexible links (*QB* and *CD*). One rigid journal is fixed to the flexible link *CD*, and another journal is fixed to the flexible link *QB*. There is a cylindrical joint with clearance between the flexible link *QB* and the ground, while the cylindrical joint that connects the two flexible links is considered to be perfect. The system is released from the initial position with null velocities and under the action of gravity acting in the negative Z-direction. In the present work, the gravitational acceleration is equal to 9.81 m/s^2. The length of each flexible link is equal to 0.5 m. The cross section of the spatial ANCF-based beam element is a square with 0.01 m side width. To avoid Poisson locking problems, the material Poisson ratio is set as zero [73]. The cylindrical joint with clearance is characterized by the bearing and journal radii equal to 0.0302 m and 0.0300 m, respectively. Thus, the joint has a radial clearance equal to 0.0002 m. The bearing and journal lengths are equal to 0.04 m. The coefficient of restitution of the contacting surfaces is assumed to be equal to 0.9. For the case of a lubricated cylindrical joint, the dynamic lubricant viscosity is chosen as 400 cP. The material density for the flexible links modeled by ANCF-based beam elements ρ is set as 2700 kg/m^3, while the material density for the rigid journal described by NCF is set as 7800 kg/m^3.

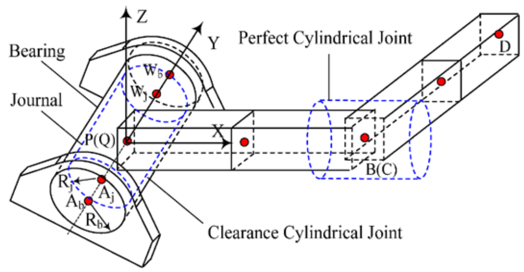

Fig. 7 Spatial double pendulum with a cylindrical clearance joint

The dynamic response of the system is quantified by the plots of displacement and velocity in the Z-direction of the point D. In addition, the trajectories of the journal centers within the bearing boundaries are also plotted. The dynamic simulations are carried out by using the cylindrical joint approaches presented in the previous sections, namely the perfect, the dry contact, and the lubricated models. The influence of the number of elements used to describe the flexible components and the effect of the Young's modulus values are also studied. Finally, with the intent to validate the proposed approaches for the stiff system, the same double pendulum model is simulated by using the commercial MSC.ADAMS software, and the corresponding results are also presented and discussed.

Figure 8 shows the influence of the number of elements and Young's modulus on the Z-displacement of point D for the case of the perfect joint model. By observing the plots, it can be concluded that for the stiff system ($E = 6.9\text{e}11$ Pa) 4 ANCF-based elements are enough to reach accurate results. For the system modeled with a material Young modulus equal to $E = 6.9\text{e}9$ Pa, 12 elements are necessary to obtain the convergent solution, while 16 elements are necessary for the very flexible system with a material Young modulus of $E = 6.9\text{e}8$ Pa.

The effect of the number of elements for the perfect and dry clearance joint models on the displacement and velocity of point D in the Z-direction is illustrated in Figs. 9 and 10. From the evolution of the plotted diagrams, one can conclude that the contact–impact phenomena that occur between the bearing and journal surfaces are more significant for the case of the flexible system, as is visible in Figs. 9c and 10c. Furthermore, for the model of cylindrical joint with clearance, some peaks on the velocity diagrams can be observed, which are clearly associated with the local relative deformation of the journal and bearing surfaces.

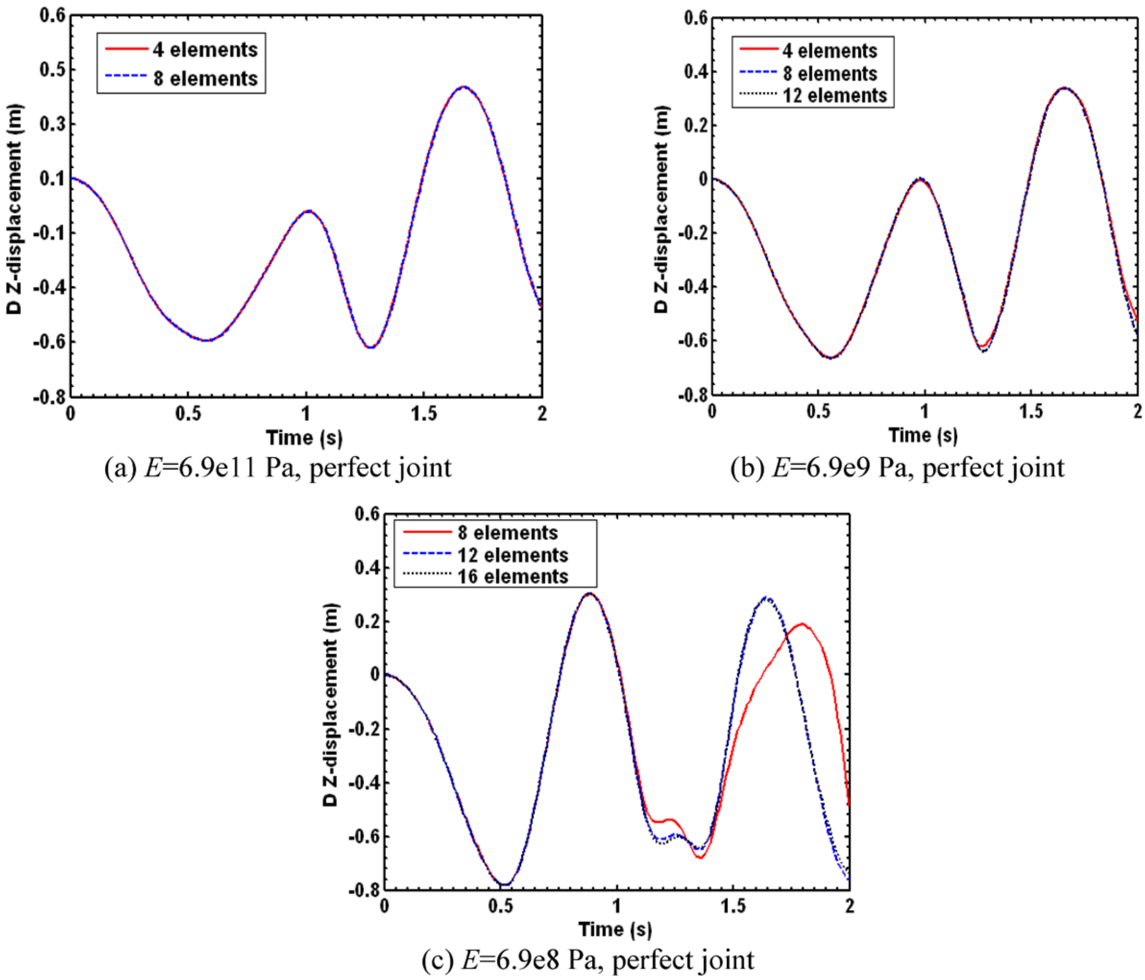

Fig. 8 Influence of number of elements used to describe the flexible bodies and material Young's modulus on the Z-displacement of point D for the perfect joint model

Again, these high-frequency sharp peaks are more important for the case in which the bodies are flexible.

Figure 11 shows the trajectories of the journal centers A_j and W_j inside the bearing boundaries for the dry clearance cylindrical joint model. In order to keep the plots simple and readable, only data relative to the first 0.5 s of simulation are presented. From the analysis of Fig. 11, different types of journal motion can be observed, namely the free flight motion, impact followed by rebound, and continuous or permanent contact between the journal and bearing surfaces. It is noteworthy that the journal misalignment phenomena are represented by the center line. Finally, one can observe the level of deformations and rebounds for the different values of material Young's modulus.

Prior to analyzing the lubricated model, it is important to validate the dry contact approach presented. For this purpose, the same double pendulum system was modeled and simulated using the commercial software MSC.ADAMS for the stiff case ($E = 6.9\text{e}11$ Pa). Figure 12 shows the plots of the Z-displacement of point D, for the perfect and dry clearance joint models obtained with the proposed methodology and with MSC.ADAMS code. In general, the plots of Fig. 12 demonstrate a good correlation of the data produced, which support the main assumptions and procedures adopted in the present work and validate the presented dry contact model.

In what follows, the results from the simulation of the double pendulum system when the clearance joint

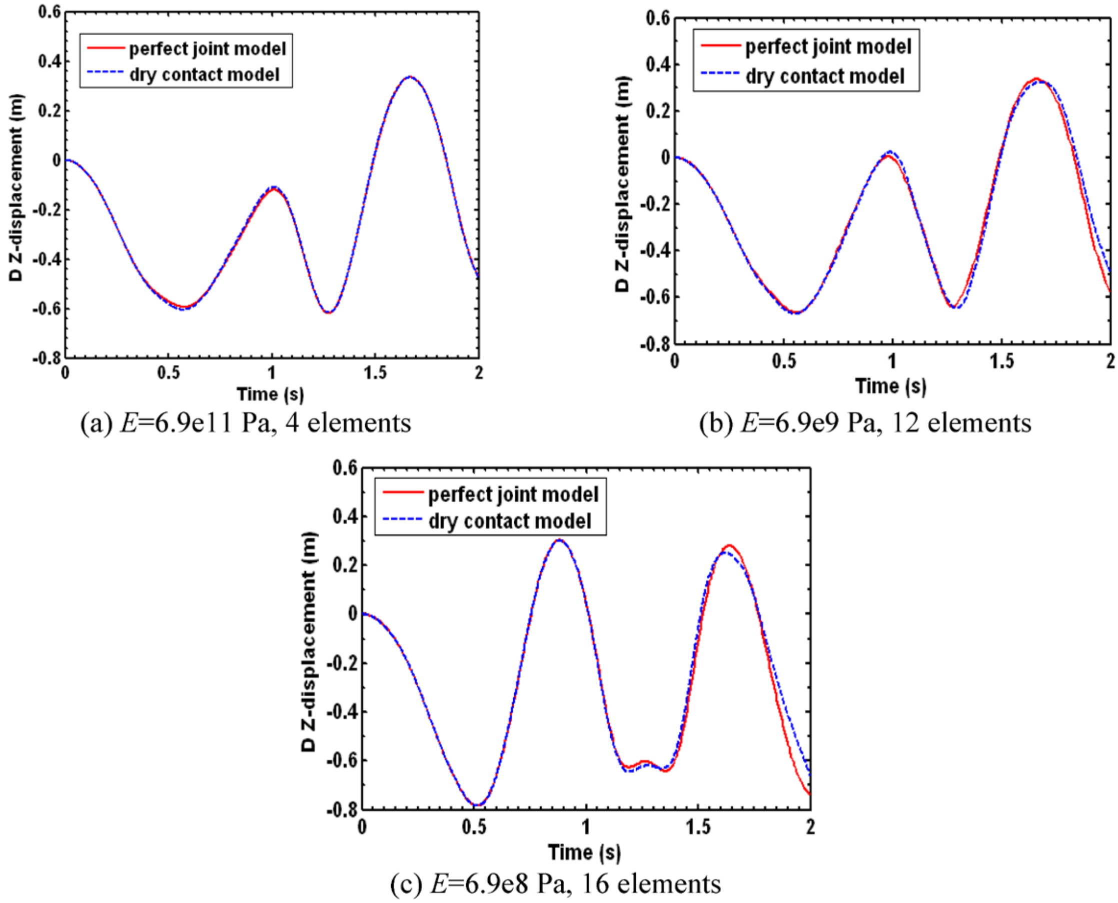

Fig. 9 Influence of number of elements used to describe the flexible bodies and material Young's modulus on the Z-displacement of point D for the perfect and dry clearance cylindrical joint models

is modeled as a lubricated joint are presented. Figures 13 and 14 show the plots of the displacement and velocity of point D in the Z-direction for the perfect and lubricated joint models, for different numbers of elements. Figure 15 illustrates the joint reaction force for perfect and lubrication joint models and for different numbers of ANCF-based elements. From these plots it can be stated that the fluid lubricant acts like a mechanical damper element since it absorbs some level of noise associated with the dry contact–impact phenomena. Hence, the global behavior for the lubricated case is closer to the situation in which the system is modeled with perfect cylindrical joints. Similar conclusions can be reached for the joint reaction forces plotted in Fig. 15.

Figure 16 presents the trajectories of the journal bases' centers A_j and W_j inside the bearing boundaries for the lubricated cylindrical joint model. In contrast to the case of the dry contact model (Fig. 11), the journal centers move closer to the corresponding bearing center, which means that there is no contact between journal and bearing surfaces due to the presence of the fluid lubricant. It should be highlighted that this phenomenon, associated with the presence of the lubricant, contributes to the extension of mechanism service life, which is also a powerful proof to illustrate the effectiveness of the proposed lubrication force formulation considering the journal misalignment. In addition, some amount of journal misalignment is visible in the plots of Fig. 16, which does not affect the global system responses.

Finally, it is important to discuss the computational efficiency of the different approaches used to model cylindrical joints. Table 1 shows the computation time

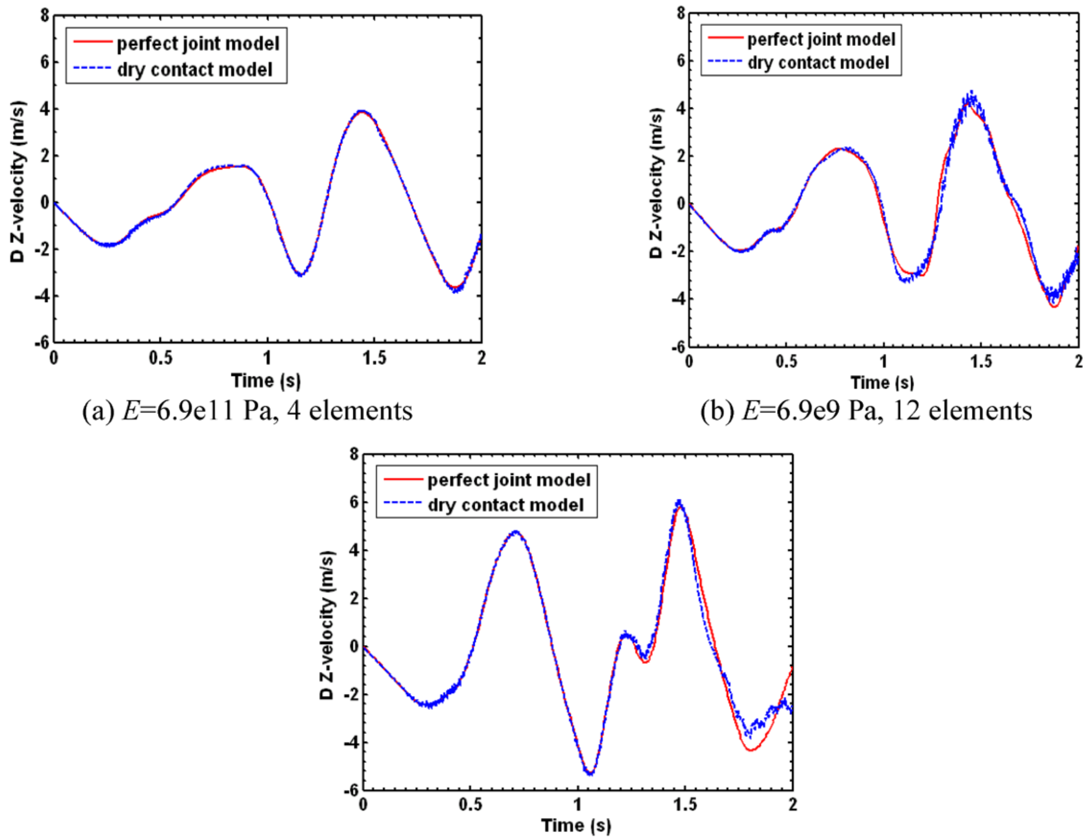

(a) E=6.9e11 Pa, 4 elements

(b) E=6.9e9 Pa, 12 elements

(c) E=6.9e8 Pa, 16 elements

Fig. 10 Influence of number of elements used to describe the flexible bodies and material Young's modulus on the Z-velocity of point D for the perfect and dry clearance cylindrical joint models

required for the three joint models considered, namely, the perfect joint model, the dry contact model, and the lubricated model. In addition, the influence of the material Young's modulus and number of elements used to describe the flexible links on the computation time is also analyzed. By observing Table 1, the first conclusion is that the computation time increases when the material Young's modulus and number of elements increase. Furthermore, when the system is modeled with perfect joints, the computational efficiency is much lower than that for the cases of dry contact and lubricated models. This fact is not surprising because the last two approaches evaluate the intra-joint forces during the dynamic simulation of the systems. In general, these conclusions are in line with those observed in the literature [29, 74]. It should be mentioned that the numerical simulations were performed on a PC with four 2.83 GHz processors and 3 GB RAM.

5.2 Spatial slider-crank mechanism

In this section, a spatial slider-crank mechanism is used as a numerical example to demonstrate the application of the methodologies previously presented. Four bodies, namely the ground, the crank, the connecting rod, and the slider, describe the slider-crank model under consideration, as illustrated in Fig. 17. The connecting rod and the slider are connected by a clearance cylindrical joint, while the remaining bodies are linked with perfect cylindrical joints. The crank, which is stiff, has a length equal to 0.05 m and a material density and Young's modulus of 6666.66 kg/m^3 and 2.07e15 Pa, respectively. Only one ANCF-based element is used to model the crank. The cross section of the beam element is a square with 0.03 m side width. In turn, the connecting rod is flexible, with a length of 0.12 m, and the material density is set as 7777.78 kg/m^3. Four elements are used to model the

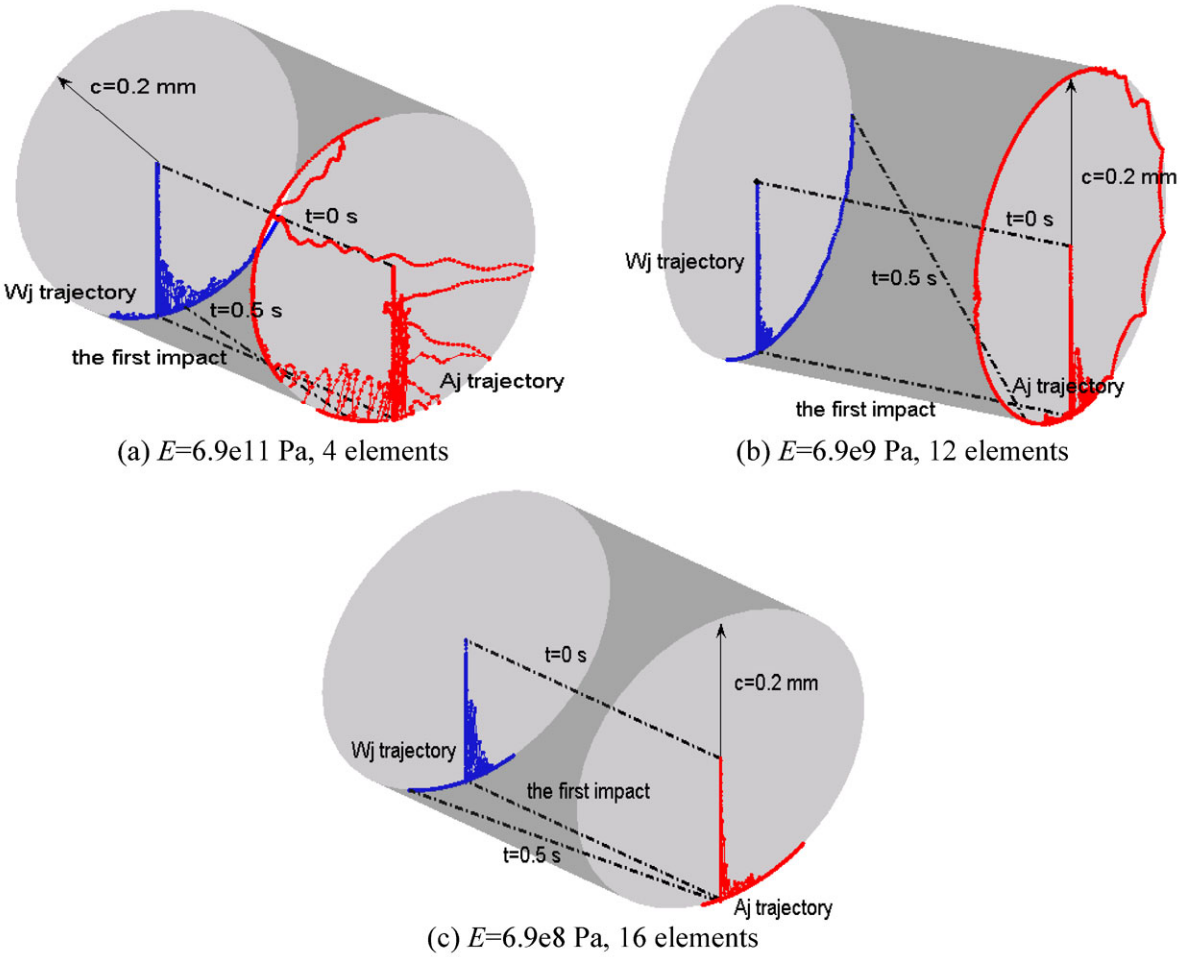

Fig. 11 Influence of number of elements used to describe the flexible bodies and material Young's modulus on journal center trajectories for the dry clearance cylindrical joint models

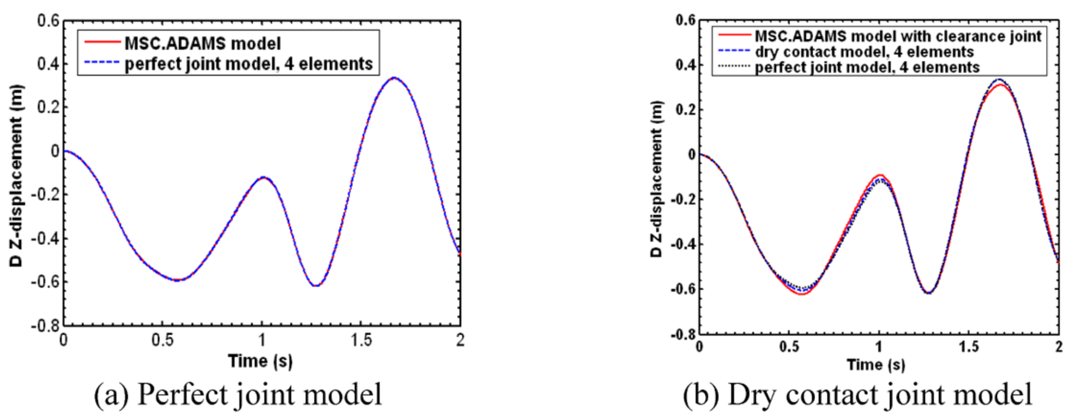

Fig. 12 Z-displacement of point D for perfect and dry contact joint models obtained with the proposed approach and by using the MSC.ADAMS code

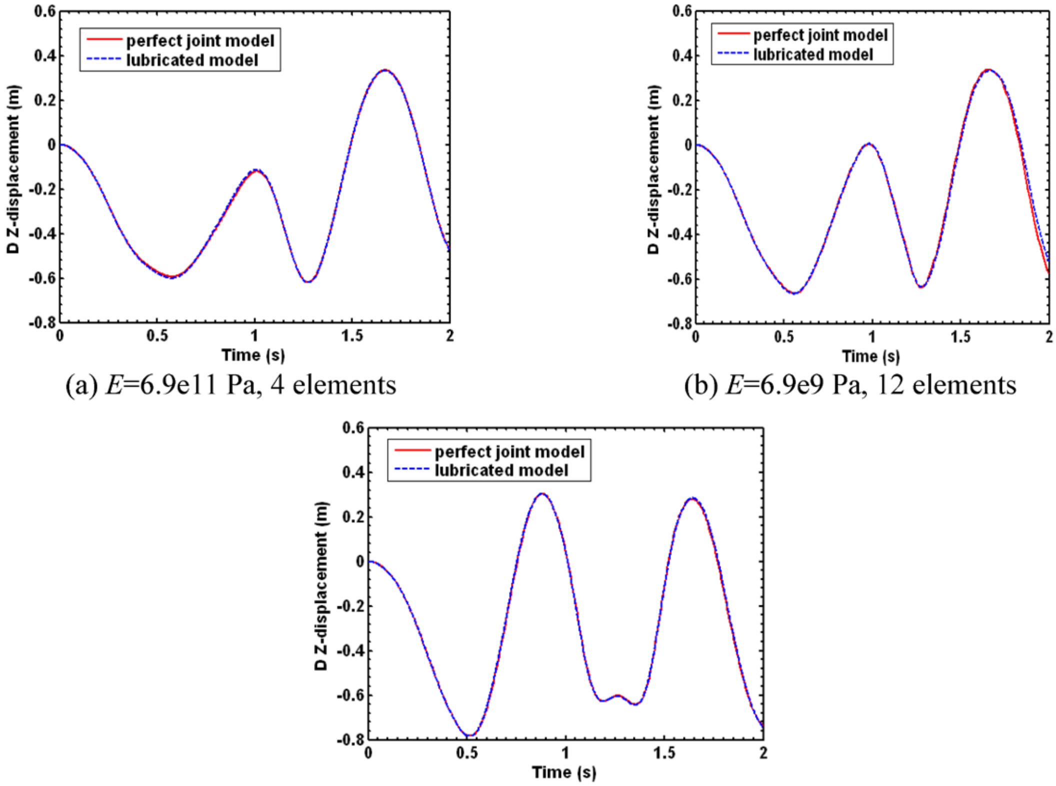

(a) E=6.9e11 Pa, 4 elements

(b) E=6.9e9 Pa, 12 elements

(c) E=6.9e8 Pa, 16 elements

Fig. 13 Influence of number of elements used to describe the flexible bodies and material Young's modulus on the Z-displacement of point D for the perfect and lubricated cylindrical joint models

Table 1 Total CPU time based on different simulation models (in seconds)

Material Young's modulus		6.9e11 Pa	6.9e9 Pa	6.9e8 Pa
Number of elements		4	12	16
Perfect joint model	Time step		$h = 2e-4$ s	
	Computation time	61 s	194 s	329 s
Dry contact model	Time step		$h = 2e-6$ s	
	Computation time	3085 s	8114 s	15,751 s
Lubricated model	Time step		$h = 2e-6$ s	
	Computation time	3885 s	10,247 s	18,114 s

connecting rod. The cross section of the beam element is a square with 0.015 m side width. In order to avoid Poisson locking problems the Poisson ratio is set to 0. The mass of the slider is equal 0.14 kg, with its moment of inertia neglected. The value of Young's modulus necessary to evaluate the contact stiffness parameter is equal to 2.07e11 Pa, with the coefficient of restitution equal to 0.9. The radius and the length of the journal are chosen as $R_j = 0.015$ m and $B = 0.02$ m, respectively. The radial clearance size is equal to 0.2 mm. For the case of the lubricated model, the dynamic fluid viscosity is equal to 400 cP. The initial configuration is taken with the crank and the connecting rod collinear. The crank, which is the driving link, rotates about the Y-axis with a constant angular velocity of 5000 rpm.

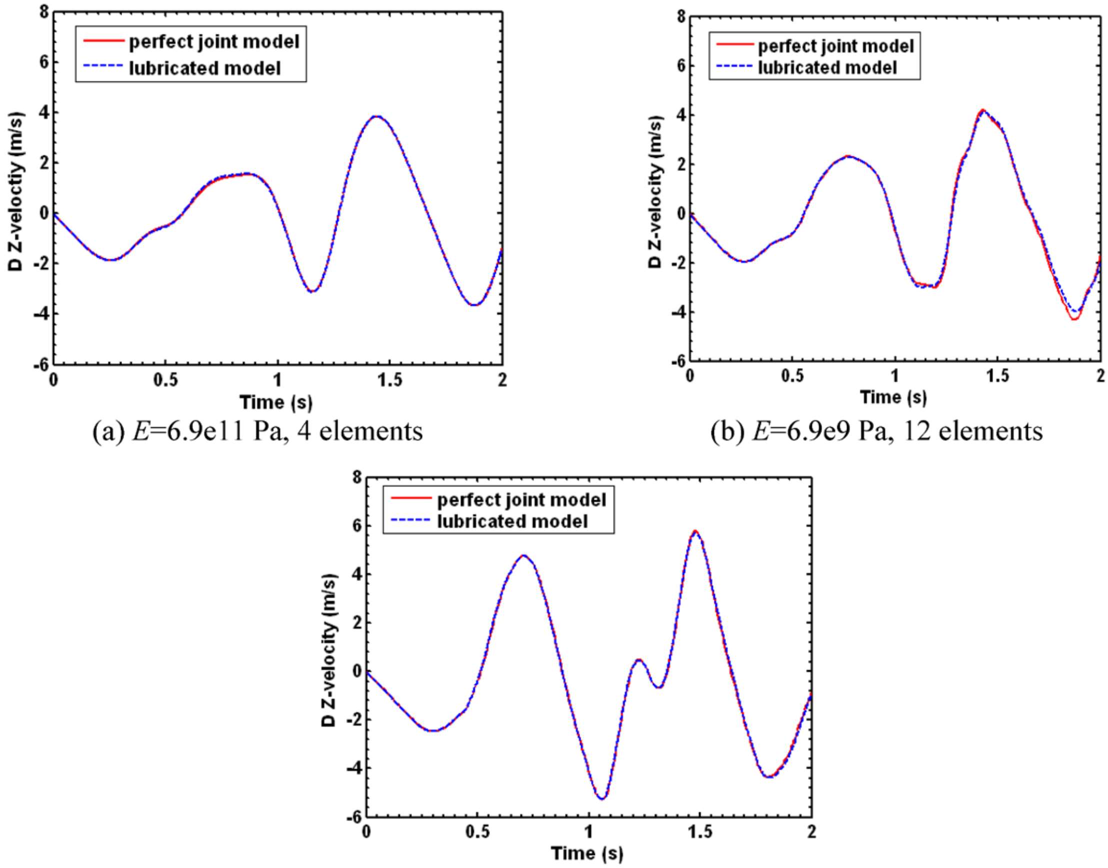

(a) E=6.9e11 Pa, 4 elements

(b) E=6.9e9 Pa, 12 elements

(c) E=6.9e8 Pa, 16 elements

Fig. 14 Influence of number of elements used to describe the flexible bodies and material Young's modulus on the Z-velocity of point D for the perfect and lubricated cylindrical joint models

Figure 18 shows the plots of the slider acceleration for the perfect and dry contact joint models when two different values of Young's modulus for the connecting rod are used. Figure 18 exhibits some peaks for the dry contact model, which can be associated with the contact–impact phenomena between the journal and bearing surfaces. Furthermore, it is also visible that the slider acceleration changes more sharply for the flexible system with material Young's modulus $E = 5\text{e}9$ Pa than for the stiff system with material Young's modulus $E = 2.07\text{e}15$ Pa. Conversely, when the lubricant fluid is introduced between the journal and bearing surfaces, the slider acceleration response is closer to the case of a perfect joint, as can be observed in the plots of Fig. 19. A similar analysis can be performed for the joint reaction forces plotted in Figs. 20 and 21.

Figure 22 shows the journal center trajectories in the clearance for the dry contact model. As was expected, the journal misalignment does not take place, as can be seen in the figure. Furthermore, it can be observed that the stiff system produces smoother trajectories, because the local deformations present a lower magnitude than for the case of the flexible system.

Figure 23 shows the paths of journal bases' centers A_j and W_j in the joint clearance for the lubricated stiff model with material Young's modulus equal to $E = 2.07\text{e}15$ Pa. It is clear that the presence of the lubricant between the journal and bearing components avoids contact between them, which is why the perfect and lubricated joint models exhibit similar behavior.

Figure 24 shows the effect of the connecting-rod flexibility on the trajectory of journal center A_j. It can be seen that the eccentricity of the journal center for the flexible system is a little larger than that of the stiff system due to the deformation of the flexible connecting rod.

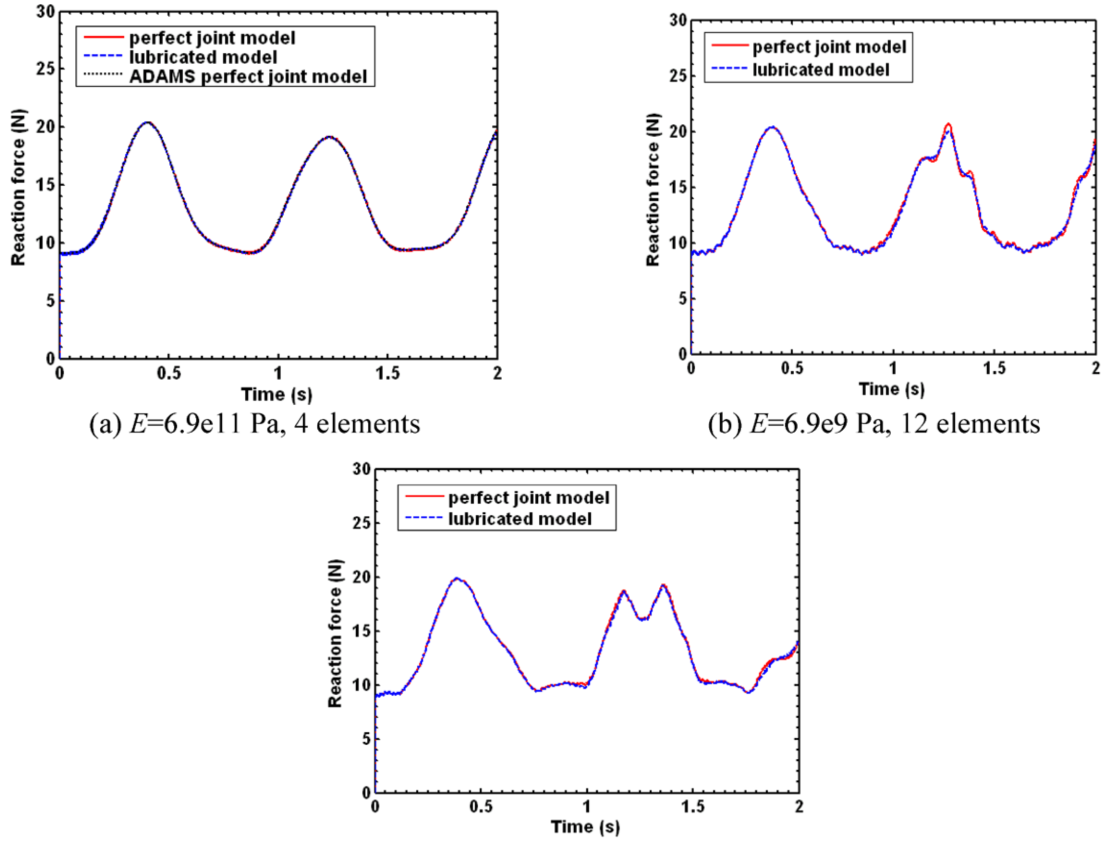

(a) E=6.9e11 Pa, 4 elements

(b) E=6.9e9 Pa, 12 elements

(c) E=6.9e8 Pa, 16 elements

Fig. 15 Influence of number of elements used to describe the flexible bodies and material Young's modulus on the joint reaction force for the perfect and lubricated cylindrical joint models

The numerical examples of application presented above lead to the following observations. The overall obtained results are in line with those of published works on this field for the case that includes the dry contact models [7, 14, 26, 37, 75, 76]. As far as the lubricated joint results are concerned, the global results are also in line with those offered in the literature [21, 22, 26, 39, 77]. The dry contact model can predict the dynamic response of a multibody system with unlubricated cylindrical joints including the peak values of the intra-joint forces as well as the deviations of the position and velocity of the bodies. These phenomena are particularly visible when bodies are modeled as flexible parts, as can be seen in Figs. 8–10, 18, and 20. The dynamic system responses are basically characterized as nonperiodic. The trajectories of the journal centers are significantly affected by the degree of the bodies' flexibility. For the case of stiff systems, the journal center trajectories exhibit different behaviors, such as impacts followed by rebounds, continuous contact between the journal and bearing surfaces, and free-flight motion. When the systems include a flexible link, the journal center trajectories tend to be limited to the continuous contact mode due to the damping effect of the bodies' elasticity. These different system responses can be observed in the plots of Fig. 11. In the case of lubricated cylindrical joints, the intra-joint reaction forces and the systems' kinematic responses are smoother and tend to be close to the case of the perfect joint model, as Figs. 13–15, 19, and 21 depict. An accurate determination of the important effects requires the proper modeling and analysis of the flexibility of the bodies. When the flexibility is neglected, the peak forces are grossly overestimated. The lubricant damping effect absorbs part of the kinetic energy and produces

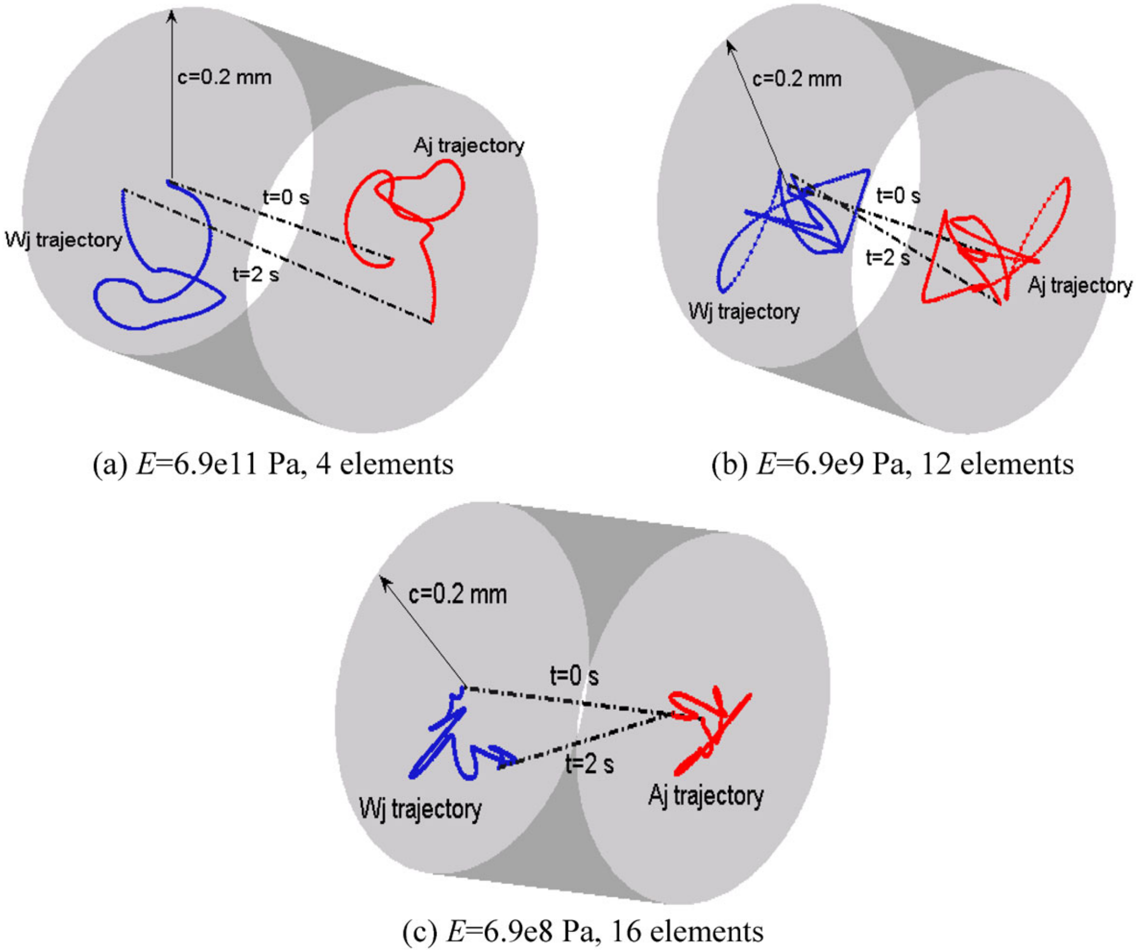

Fig. 16 Influence of number of elements used to describe the flexible bodies and material Young's modulus on journal center trajectories for the lubricated cylindrical joint models

Fig. 17 Spatial slider-crank mechanism with a cylindrical clearance joint

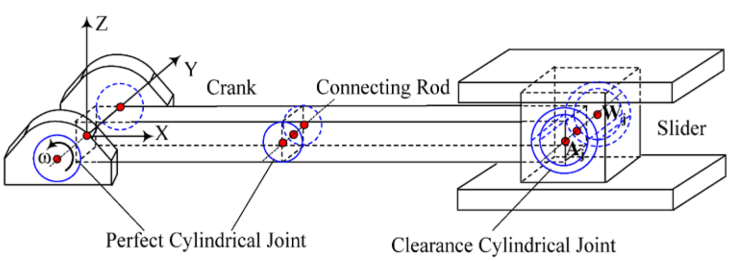

smoother and periodic system responses. It must be emphasized that the inclusion of a flexible link in the system, combined with a clearance joint, can lead to large deformation and, consequently, produce higher joint reaction forces, as illustrated in Fig. 21. It is obvious that the presence of lubricant avoids direct contact between the journal and bearing surfaces. However, some numerical difficulties can arise when the system includes high eccentricity and/or low fluid viscosity. This makes sense from a physical point of view, as in these cases the hydrodynamic lubrication theory is not valid and must be substituted by the elasto-hydrodynamic approach, which is out of the scope of the present work. Moreover, the proposed method-

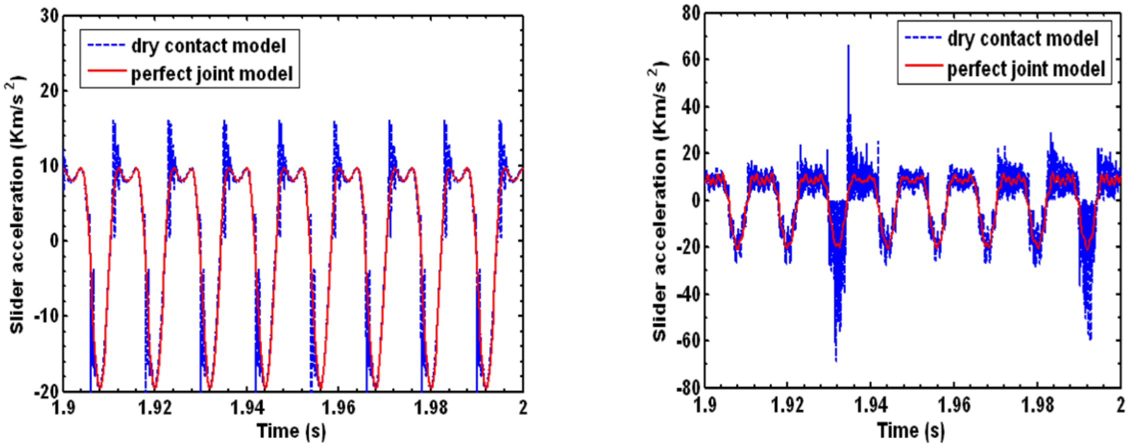

(a) E=2.07e15 Pa (b) E=5e9 Pa

Fig. 18 Slider acceleration for the perfect and dry clearance cylindrical joint models

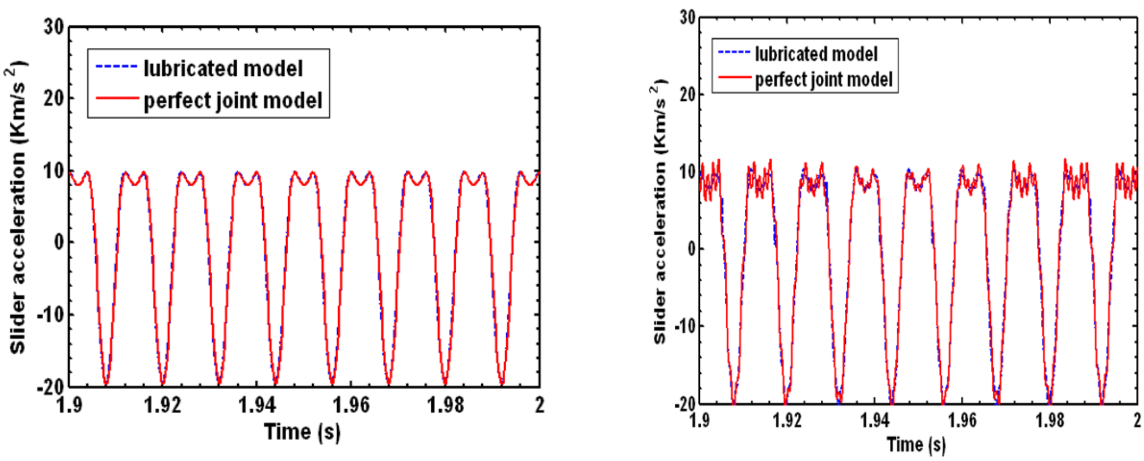

(a) E=2.07e15 Pa (b) E=5e9 Pa

Fig. 19 Slider acceleration for the perfect and lubricated cylindrical joint models

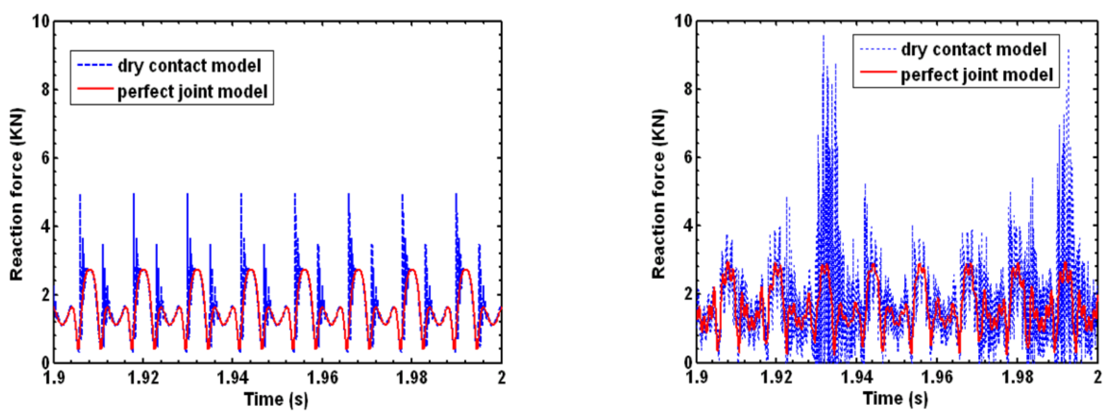

(a) E=2.07e15 Pa (b) E=5e9 Pa

Fig. 20 Joint reaction force for the perfect and dry clearance cylindrical joint models

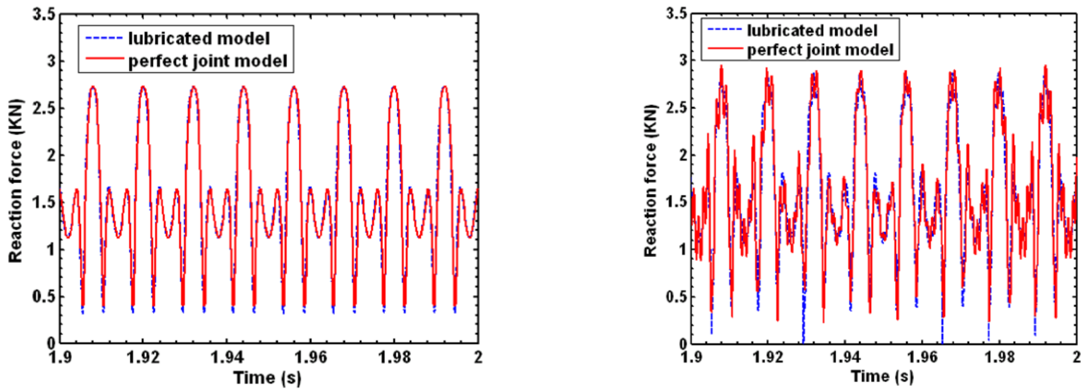

(a) E=2.07e15 Pa (b) E=5e9 Pa

Fig. 21 Joint reaction force for the perfect and lubricated cylindrical joint models

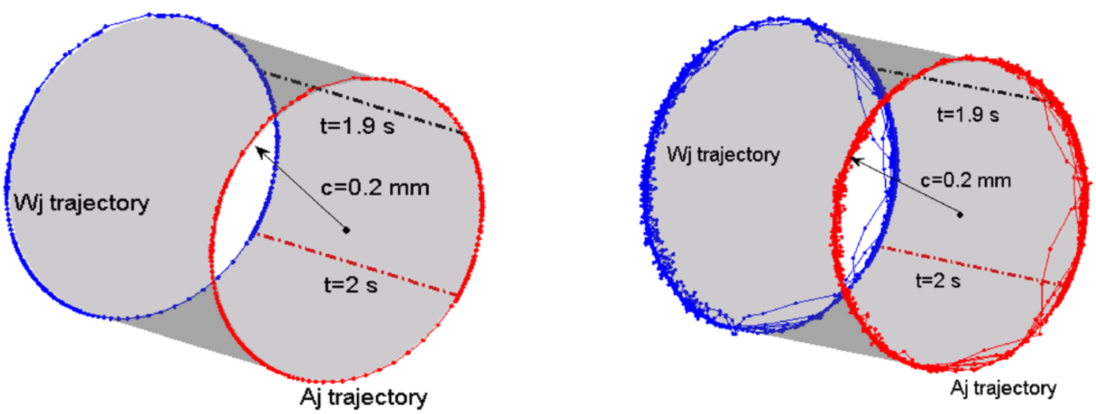

(a) E=2.07e15 Pa (b) E=5e9 Pa

Fig. 22 The paths of journal centers A_j and W_j in the joint clearance for dry contact models (1.9–2 s)

ology is able to accommodate some amount of misalignment between the journal and bearing axis. This particular issue has not been addressed before in the literature. In short, for real multibody systems, clearance, lubrication, and elasticity phenomena are always present and can significantly affect the dynamic responses of the systems. Therefore, the ability to model these phenomena plays a key role in accurately predicting the dynamic response of mechanical systems, and also has consequences in the design process. From this point of view, all the models proposed are able to capture the different phenomena involved in the dynamics of flexible spatial multibody systems that include cylindrical joints with clearance and lubrication effects.

6 Conclusions

Based on the absolute nodal coordinate formulation (ANCF) and the natural coordinate formulation (NCF), a new general and comprehensive approach for a spatial flexible multibody system with cylindrical clearance joint has been derived. The flexible parts are described by the ANCF, while the rigid journals are described by the NCF. The resulting mass matrix in the final system equations of motion is constant, which benefits the computational efficiency. For both dry contact and lubrication conditions, the journal misalignment is considered. The dry contact–impact forces due to the collisions of the bodies are computed by using a modified Hertzian-based continuous contact law, while the lubrication forces are directly ob-

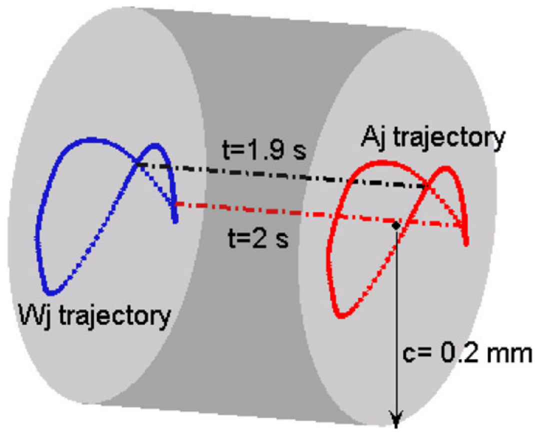

Fig. 23 The paths of journal centers A_j and W_j in the joint clearance for lubricated models ($E = 2.07\text{e}15$ Pa, $t = 1.9$–2 s)

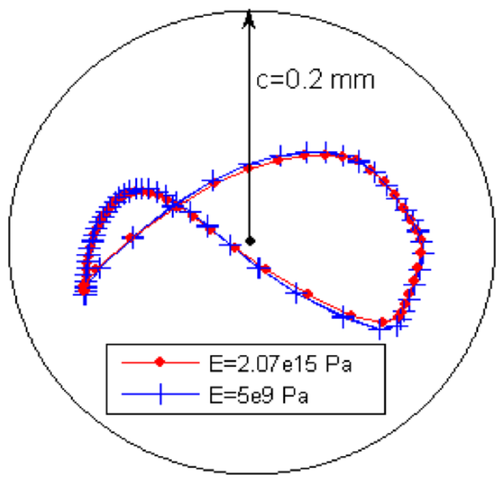

Fig. 24 The paths of journal centers A_j in the joint clearance for lubricated models ($E = 2.07\text{e}15$ Pa, $t = 1.9$–2 s)

tained from the Reynolds equation based on the short journal-bearing approach. The effects of the material Young's modulus of the flexible parts on the system's dynamic responses are investigated. To dissipate the system high-frequency responses and preserve the low-frequency responses, the generalized-$\boldsymbol{\alpha}$ method is used to solve the equations of motion. In order to validate the methodology presented in this paper, some results are compared to those obtained by using the software MSC.ADAMS. In addition, the obtained results are also compared with those published in the literature. It was shown that the fluid lubricant can avoid or greatly reduce the direct bearing-journal impact. All the results indicate that the modeling methods and the lubrication forces formulations for the flexible multibody systems with dry and lubricated cylindrical clearance joints are effective. Furthermore, developments of the present research work can include surface roughness and wear phenomena.

Acknowledgements This work is supported by the subproject of China "973" project (613117) and a key CAST project (CAST200911) from China Academy of Space Technology and by the Portuguese Foundation for the Science and Technology under the research project BIOJOINTS (PTDC/EME-PME/099764/2008). The third author expresses her gratitude to FCT for the Ph.D. grant SFRH/BD/40164/2007. Finally, we want to express our sincere thanks to Prof. Daniel García-Vallejo from University of Seville, Spain, and Dr. Johannes Gerstmayr from Johannes Kepler University of Linz, Austria, for their very valuable help with the ANCF method.

References

1. Nikravesh, P.E.: Computer-Aided Analysis of Mechanical Systems. Prentice-Hall, New York (1988)
2. Haug, E.J.: Computer-Aided Kinematics and Dynamics of Mechanical Systems, Basic Methods, vol. I. Allyn & Bacon, Needham Heights (1989)
3. Shabana, A.A.: Dynamics of Multibody Systems. Wiley, New York (1989)
4. Flores, P., Claro, J.C.P.: A systematic and general approach to kinematic position errors due to manufacturing and assemble tolerances. In: Proceedings of ASME 2007 International Design Engineering Technical Conferences and Computers and Information in Engineering Conference, Las Vegas, NV, 4–7 September (2007). 7 pp.
5. Mukras, S., Kim, N.H., Mauntler, N.A., Schmitz, T.L., Sawyer, W.G.: Analysis of planar multibody systems with revolute joint wear. Wear **268**(5–6), 643–652 (2010)
6. Bing, S., Ye, J.: Dynamic analysis of the reheat-stop-valve mechanism with revolute clearance joint in consideration of thermal effect. Mech. Mach. Theory. **43**(12), 1625–1638 (2008)
7. Flores, P., Ambrósio, J., Claro, J.C.P., Lankarani, H.M.: Kinematics and dynamics of multibody systems with imperfect joints: models and case studies. In: Lecture Notes in Applied and Computational Mechanics, vol. 34. Springer, Berlin (2008)
8. Bu, W., Liu, Z., Tan, J., Gao, S.: Detachment avoidance of joint elements of a robotic manipulator with clearances based on trajectory planning. Mech. Mach. Theory **45**, 925–940 (2010)
9. Ambrósio, J., Veríssimo, P.: Improved bushing models for general multibody systems and vehicle dynamics. Multibody Syst. Dyn. **22**, 341–365 (2009)
10. Machado, M., Flores, P., Claro, J.C.P., Ambrósio, J., Silva, M., Completo, A., Lankarani, H.M.: Development of a planar multi-body model of the human knee joint. Nonlinear Dyn. **60**(3), 459–478 (2010)
11. Dubowsky, S., Freudenstein, F.: Dynamic analysis of mechanical systems with clearances, part 1: formulation of dynamic model. J. Eng. Ind. **93**(1), 305–309 (1971)

12. Dubowsky, S., Freudenstein, F.: Dynamic analysis of mechanical systems with clearances, part 2: dynamics response. J. Eng. Ind. **93**(1), 310–316 (1971)
13. Miedema, B., Mansour, W.M.: Mechanical joints with clearance: a three-mode model. J. Eng. Ind. **98**(4), 1319–1323 (1976)
14. Flores, P., Ambrósio, J.: Revolute joints with clearance in multibody systems. Comput. Struct. **82**, 1359–1369 (2004)
15. Erkaya, S., Uzmay, İ.: A neural-genetic (NN–GA) approach for optimising mechanisms having joints with clearance. Multibody Syst. Dyn. **20**, 69–83 (2008)
16. Flores, P., Ambrósio, J., Claro, J.C.P., Lankarani, H.M.: Translational joints with clearance in rigid multibody systems. J. Comput. Nonlinear Dyn. **3**, 0110071 (2008)
17. Erkaya, S., Uzmay, İ.: Determining link parameters using genetic algorithm in mechanisms with joint clearance. Mech. Mach. Theory **44**, 222–234 (2009)
18. Flores, P.: Modeling and simulation of wear in revolute clearance joints in multibody systems. Mech. Mach. Theory **44**, 1211–1222 (2009)
19. Erkaya, S., Uzmay, I.: Investigation on effect of joint clearance on dynamics of four-bar mechanism. Nonlinear Dyn. **58**(1–2), 179–198 (2009)
20. Duarte, F.B., Tenreiro, J.: Describing function of two masses with backlash. Nonlinear Dyn. **56**(4), 409–413 (2009)
21. Tian, Q., Zhang, Y., Chen, L., Flores, P.: Dynamics of spatial flexible multibody systems with clearance and lubricated spherical joints. Comput. Struct. **87**, 913–929 (2009)
22. Flores, P., Lankarani, H.M.: Spatial rigid-multi-body systems with lubricated spherical clearance joints: modeling and simulation. Nonlinear Dyn. **60**(1–2), 99–114 (2010)
23. Roger, R.J., Andrews, G.C.: Dynamic simulation of planar mechanical systems with lubricated bearing clearances using vector-network methods. J. Eng. Ind. **99**(1), 131–137 (1977)
24. Liu, T.S., Lin, Y.S.: Dynamic analysis of flexible linkages with lubricated joints. J. Sound Vib. **141**(2), 193–205 (1990)
25. Ravn, P., Shivaswamy, S., Alshaer, B.J., Lankarani, H.M.: Joint clearances with lubricated long bearings in multibody mechanical systems. J. Mech. Des. **122**, 484–488 (2000)
26. Schwab, A.L., Meijaard, J.P., Meijers, P.: A comparison of revolute joint clearance model in the dynamic analysis of rigid and elastic mechanical systems. Mech. Mach. Theory. **37**(9), 895–913 (2002)
27. Moes, H., Sikkes, E.G., Bosma, R.: Mobility and impedance tensor methods for full and partial-arc journal bearings. J. Tribol. **108**, 612–620 (1986)
28. Flores, P., Ambrósio, J., Claro, J.C.P., Lankarani, H.M., Koshy, C.S.: Lubricated revolute joints in rigid multibody systems. Nonlinear Dyn. **56**, 277–295 (2009)
29. Tian, Q., Zhang, Y., Chen, L., Yang, J.: Simulation of planar flexible multibody systems with clearance and lubricated revolute joints. Nonlinear Dyn. **60**, 489–511 (2010)
30. Stefanelli, R., Valentini, P.P., Vita, L.: Modeling of hydrodynamic journal bearing in spatial multibody systems. In: ASME International Design Engineering Technical Conference, DETC2005-84858, CA (2005)
31. García De Jalón, J., Bayo, E.: Kinematic and Dynamic Simulation of Multibody Systems: The Real-Time Challenge. Springer, New York (1994)
32. Shabana, A.A., Yakoub, R.Y.: Three-dimensional absolute nodal coordinate formulation for beam elements: theory. J. Mech. Des. **123**, 606–613 (2001)
33. Yakoub, R.Y., Shabana, A.A.: Three-dimensional absolute nodal coordinate formulation for beam elements: implementation and applications. J. Mech. Des. **123**, 614–621 (2001)
34. Sopanen, J.T., Mikkola, A.M.: Description of elastic forces in absolute nodal coordinate formulation. Nonlinear Dyn. **34**, 53–74 (2003)
35. Schwab, A.L., Meijaard, J.P.: Comparison of three-dimensional flexible beam elements for dynamic analysis: classical finite element formulation and absolute nodal coordinate formulation. J. Comput. Nonlinear Dyn. **5**, 0110101 (2010)
36. García-Vallejo, D., Mayo, J., Escalona, J.L., Domínguez, J.: Three-dimensional formulation of rigid-flexible multibody systems with flexible beam elements. Multibody Syst. Dyn. **20**, 1–28 (2008)
37. Flores, P., Ambrósio, J., Claro, J.C.P., Lankarani, H.M.: Spatial revolute joints with clearances for dynamic analysis of multibody systems. Proc. Inst. Mech. Eng. Part K, J. Multi-body Dyn. **220**(4), 257–271 (2006)
38. Gilardi, G., Sharf, I.: Literature survey of contact dynamics modelling. Mech. Mach. Theory **37**, 1213–1239 (2002)
39. Flores, P., Ambrósio, J., Claro, J.P.: Dynamic analysis for planar multibody mechanical systems with lubricated joints. Multibody Syst. Dyn. **12**, 47–74 (2004)
40. Flores, P., Ambrósio, J., Claro, J.C.P., Lankarani, H.M.: Influence of the contact–impact force model on the dynamic response of multibody systems. Proc. Inst. Mech. Eng, Part K, J. Multi-body Dyn. **220**(1), 21–34 (2006)
41. Lankarani, H.M., Nikravesh, P.E.: A contact force model with hysteresis damping for impact analysis of multibody systems. J. Mech. Des. **112**, 369–376 (1990)
42. Hunt, K.H., Crossley, F.R.E.: Coefficient of restitution interpreted as damping in vibroimpact. J. Appl. Mech. **7**, 440–445 (1975)
43. Dietl, P., Wensing, J., van Nijen, G.C.: Rolling bearing damping for dynamic analysis of multi-body systems-experimental and theoretical results. Proc. Inst. Mech. Eng. Part K, J. Multi-body Dyn. **214**(1), 33–43 (2000)
44. Goldsmith, W.: Impact, the Theory and Physical Behaviour of Colliding Solids. Edward Arnold Ltd, London (1960)
45. Love, A.E.H.: A Treatise on the Mathematical Theory of Elasticity, 4th edn. Dover, New York (1944)
46. Stronge, W.J.: Impact Mechanics. Cambridge University Press, Cambridge (2000)
47. Lankarani, H.M., Nikravesh, P.E.: Continuous contact force models for impact analysis in multibody systems. Nonlinear Dyn. **5**, 193–207 (1994)
48. Hippmann, G.: An algorithm for compliant contact between complexly shaped bodies. Multibody Syst. Dyn. **12**, 345–362 (2004)
49. Gonthier, Y., McPhee, J., Lange, C., Piedboeuf, J.-C.: A regularized contact model with asymmetric damping and dwell-time dependent friction. Multibody Syst. Dyn. **11**, 209–233 (2004)
50. Bei, Y., Fregly, B.J.: Multibody dynamic simulation of knee contact mechanics. Med. Eng. Phys. **26**, 777–789 (2004)

51. Dopico, D., Luaces, A., Gonzalez, M., Cuadrado, J.: Dealing with multiple contacts in a human-in-the-loop application. In: Arczewski, K., Frączek, J., Wojtyra, M. (eds.) Proceedings of Multibody Dynamics 2009, ECCOMAS Thematic Conference Warsaw, Poland, June 29–July 2 (2009), 17 pp.
52. Pereira, C.M., Ambrósio, J.A., Ramalho, A.L.: A methodology for the generation of planar models for multibody chain drives. Multibody Syst. Dyn. **23**, 303–324 (2010)
53. Flores, P., Leine, R., Glocker, C.: Modeling and analysis of planar rigid multibody systems with translational clearance joints based on the non-smooth dynamics approach. Multibody Syst. Dyn. **23**, 165–190 (2010)
54. Ahmed, S., Lankarani, H.M., Pereira, M.F.O.S.: Frictional impact analysis in open loop multibody mechanical system. J. Mech. Des. **121**, 119–127 (1999)
55. Greenwood, D.T.: Principles of Dynamics. Prentice-Hall, New York (1965)
56. Ambrósio, J.A.C.: Impact of rigid and flexible multibody systems: Deformation description and contact models. In: Schiehlen, W., Valásek, M. (eds.) Proceedings of the NATO-ASI on Virtual Non-linear Multibody Systems, vol. II, pp. 15–33 (2002)
57. Karnopp, D.: Computer simulation of stick-slid friction in mechanical dynamic systems. J. Dyn. Syst., Meas. Control **107**, 100–103 (1985)
58. Centea, D., Rahnejat, H., Menday, M.T.: Non-linear multibody dynamic analysis for the study of clutch torsional vibrations (judder). Appl. Math. Model. **25**, 177–192 (2001)
59. Haessig, D.A., Friedland, B.: On the modelling and simulation of friction. J. Dyn. Syst., Meas. Control **113**, 354–362 (1991)
60. García De Jalón, J., Bayo, E.: Kinematic and Dynamic Simulation of Multibody Systems the Real-Time Challenge. Springer, New York (1994)
61. Hori, Y.: Hydrodynamic Lubrication. Springer, Berlin (2006)
62. Goenka, P.K.: Effect of surface ellipticity on dynamically loaded spherical and cylindrical joints and bearings. Ph.D. Dissertation, Cornell University, Ithaca, New York (1980)
63. Pinkus, O., Sternlicht, S.A.: Theory of Hydrodynamic Lubrication. McGraw-Hill, New York (1961)
64. Shabana, A.A.: Computational Dynamics, 3rd edn. Wiley, New York (2010)
65. Hussein, B., Negrut, D., Shabana, A.A.: Implicit and explicit integration in the solution of the absolute nodal coordinate differential/algebraic equations. Nonlinear Dyn. **54**, 283–296 (2008)
66. Tian, Q., Zhang, Y., Chen, L., Yang, J.: An efficient hybrid method for multibody dynamics simulation based on absolute nodal coordinate formulation. J. Comput. Nonlinear Dyn. **4**, 021009 (2009)
67. Shabana, A.A., Hussein, B.: A two-loop sparse matrix numerical integration procedure for the solution of differential/algebraic equations: application to multibody systems. J. Sound Vib. **327**, 557–563 (2009)
68. Chung, J., Hulbert, G.: A time integration algorithm for structural dynamics with improved numerical dissipation: the generalized-α method. J. Appl. Mech. **60**, 371–375 (1993)
69. Gerstmayr, J., Shabana, A.A.: Efficient integration of the elastic forces and thin three-dimensional beam elements in the absolute nodal coordinate formulation. In: ECCOMAS Thematic Conference, Madrid, Spain, 21–24 June (2005)
70. Gerstmayr, J.: A solution strategy for elasto-plastic multibody systems and related problems. Ph.D. Dissertation, University of Linz, Austria (2001)
71. Flores, P., Ambrósio, P.: On the contact detection for contact–impact analysis in multibody systems. Multibody Syst. Dyn. **24**, 103–122 (2010)
72. Meijaard, J.P.: Efficient numerical integration of the equations of motion of non-smooth mechanical systems. Z. Angew. Math. Mech. **77**, 419–427 (1997)
73. Sopanen, J.T., Mikkola, A.M.: Description of elastic forces in absolute nodal coordinate formulation. Nonlinear Dyn. **34**, 53–74 (2003)
74. Flores, P.: A parametric study on the dynamic response of planar multibody systems with multiple clearance joints. Nonlinear Dyn. **61**, 633–653 (2010)
75. Kakizaki, T., Deck, J.F., Dubowsky, S.: Modeling the spatial dynamics of robotic manipulators with flexible links and joint clearances. J. Mech. Des. **115**, 839–847 (1993)
76. Orden, J.C.G.: Analysis of joint clearances in multibody systems. Multibody Syst. Dyn. **13**(4), 401–420 (2005)
77. Bauchau, O.A., Rodriguez, J.: Modelling of joints with clearance in flexible multibody systems. Int. J. Solids Struct. **39**, 41–63 (2002)